

See discussions, stats, and author profiles for this publication at: <https://www.researchgate.net/publication/314246409>

Inkjet printing wearable electronic devices

Article in *Journal of Materials Chemistry C* · January 2017

DOI: 10.1039/C7TC00038C

CITATIONS

247

READS

2,813

3 authors:



Meng Gao

Tianjin University of Science and Technology

20 PUBLICATIONS 745 CITATIONS

[SEE PROFILE](#)



Lihong Li

Chinese Academy of Sciences

44 PUBLICATIONS 1,810 CITATIONS

[SEE PROFILE](#)



Yanlin Song

Chinese Academy of Sciences

555 PUBLICATIONS 23,965 CITATIONS

[SEE PROFILE](#)

Some of the authors of this publication are also working on these related projects:



51473173 [View project](#)



perovskite solar cell [View project](#)



CrossMark
click for updates

Cite this: DOI: 10.1039/c7tc00038c

Inkjet printing wearable electronic devices

Meng Gao,^{ab} Lihong Li^{*a} and Yanlin Song^{*a}

Received 4th January 2017,
Accepted 18th February 2017

DOI: 10.1039/c7tc00038c

rsc.li/materials-c

In recent years, wearable electronics have experienced tremendous development due to their promising applications in fields such as portable, flexible/stretchable human-interactive sensors, displays, and energy devices. To effectively fabricate wearable electronics, a high-efficient, cost-saving, and eco-friendly manufacture technology is required. Inkjet printing, which rapidly, precisely, and reproducibly deposits a broad variety of functional materials in a non-impact, additive patterning, and maskless approach, serves as an effective tool for the fabrication of wearable electronics. In this review, the recent advances in inks, strategies, and the applications of inkjet-printed wearable electronics are summarized. Based on uniform and high-resolution patterns, well-compatible functional inks can be deposited to fabricate flexible/stretchable and durable wearable electronics. Perspectives on the remaining challenges and future developments are also proposed.

1. Introduction

Wearable electronic devices have recently attracted significant attention due to their facile interaction with humans.^{1–6} These devices can be attached onto clothes or even directly mounted onto human skin for applications such as portable displays, human activity monitoring sensors, and self-powered devices. Wearable displays could enable the development of expandable and foldable screens for smartphones, electronic clothes, and rollable or collapsible wallpaper-like display boards. Wearable

sensors can also play an important role in detecting and monitoring the physical, chemical, biological, and environmental status of the human body with high efficiency and minimum discomfort. Wearable energy devices, which contribute to portable self-powered device manufacturing, provide convenience for wireless and long-lasting utilization of electronics associated with human beings. Traditionally, wearable electronic devices have been mainly manufactured by photolithography, vacuum deposition, and electroless plating processes.⁷ However, all these methods suffer from disadvantages including multi-staged procedures, high-cost equipment, and the production of large amounts of environmentally undesirable waste.

As alternatives, printing techniques, including screen printing, gravure printing/imprinting, flexographic printing, roll-to-roll printing and inkjet printing, are prominently being developed to promote scalable and effective electronic manufacturing.

^a Key Laboratory of Green Printing, Institute of Chemistry, Chinese Academy of Sciences, Beijing 100190, P. R. China. E-mail: lilihong1209@iccas.ac.cn, ylsong@iccas.ac.cn

^b School of Chemistry and Chemical Engineering, University of Chinese Academy of Sciences, Beijing 100049, P. R. China



Meng Gao

Meng Gao is currently a PhD candidate at the Institute of Chemistry, Chinese Academy of Sciences (ICCAS). She received her BS degree in Polymer Science and Technology from Beijing University of Chemical Technology, China, in 2012. Then, she joined Prof. Yanlin Song's group at ICCAS. Her current scientific interest is focused on self-powered devices, wearable electronics and the green printing of functional materials.



Lihong Li

Lihong Li received her BS degree from Wuhan University of Science and Technology in June 2005 and her PhD from University of Science and Technology Beijing (USTB) in Jan 2011. She carried out her post-doctoral research at Tsinghua University, in 2011. She is now an associate professor of the Institute of Chemistry, Chinese Academy of Sciences. Her research interests are inorganic functional materials, material chemistry and the green printing of nano functional inks.

Among these, inkjet printing, which accurately deposits micro- and nanomaterials into functional arrangement in a non-impact, additive patterning and maskless approach, has aroused great attention in recent years.^{8–14} With the virtue of its low-cost, easily changeable digital print patterns and low material consumption, inkjet printing has been widely used in fabricating electronics, including thin film transistors (TFTs),^{15,16} transparent electrodes,¹⁷ sensors,^{18,19} solar cells,^{20,21} electroluminescent displays²² and complementary ring oscillators.²³ Since wearable electronics are required to meet a number of key requirements, including high flexibility/stretchability, high durability, biocompatibility and lightweight, it is crucial to take the following key components into consideration when performing inkjet printing: (i) the use of non-toxic, highly soluble, chemically stable, low-temperature processable inks for smooth inkjet printing and compatible post-treatment, (ii) uniform and high-resolution patterns for excellent electrical properties and a high integration of lightweight devices, (iii) the use of flexible/stretchable substrates for electronic devices to be worn or integrated with the human body, (iv) particular design of the device structure to prohibit cracking and slipping for high durability of device usage. Thus, by deliberately controlling the inkjet-printing procedure, high-performance wearable electronics can be manufactured.

In this review, we summarize and discuss the progress in inks, strategies and the applications of inkjet-printed wearable electronics (Fig. 1).^{24–35} Inks consisting of conductors, semiconductors and dielectrics are presented in view of meeting the requirements of both the inkjet-printing procedure and wearable electronics manufacture, followed with an introduction of the critical parameters for ink printability. Then, we discuss the strategies to inkjet print wearable devices with high-quality patterns, high flexibility/stretchability and durability. Furthermore, applications of inkjet-printed wearable devices are introduced. Finally, perspectives on the future developments and remaining challenges in this field are discussed.



Yanlin Song

materials, photonic crystals, printed electronics and green printing materials and technologies.

Yanlin Song received his PhD degree from the Department of Chemistry at Peking University in 1996. He then worked as a postdoctoral fellow in the Department of Chemistry of Tsinghua University from 1996 to 1998. He joined the Institute of Chemistry, Chinese Academy of Sciences, in 1998. He is currently a professor and director of Key Laboratory of Green Printing, Chinese Academy of Sciences. His research interests include information function

2. Inks for wearable electronics

Inks with typical functional materials and various additives (such as rheology and surface tension modifiers, humectants, binders and defoamers) dissolved or dispersed in a liquid vehicle (aqueous or organic solvent) represent the fundamental platform for the optimal performance of printing. Stable printability is a prerequisite for printing well-generated droplets and reliable patterns. It is a fundamental issue for inkjet printing, and will be discussed in the ink printability section. For specific materials, requirements such as high solubility of functional materials, high chemical stability and high electronic performance with acceptable cost and a convenient synthesis procedure can ensure high-performance device fabrication with reasonable inputs. Since wearable electronics tend to involve an intimate association with humans, biocompatibility and low-temperature processability are significant for operational safety and device flexibility, which should also be taken into account when preparing inks. Strategies to satisfy the requirements mentioned above for specific materials will be discussed in the section covering the ink deposition of functional materials.

2.1 Ink printability

To form reliable patterns orderly during printing, an individual droplet should be stably generated without long tails and satellites. The representative characteristic dimensionless numbers that affect the behaviour of the ink are the Reynolds number (Re),³⁶ Weber number (We)³⁷ and Ohnesorge number (Oh):³⁸

$$\text{Re} = \frac{\nu\rho\alpha}{\eta}$$

$$\text{We} = \frac{\nu^2\rho\alpha}{\gamma}$$

$$\text{Oh} = \frac{\sqrt{\text{We}}}{\text{Re}} = \frac{\eta}{(\gamma\rho\alpha)}$$

where ν , α , ρ , η and γ represent the velocity, characteristic length (typically drop diameter), density, viscosity and surface tension of the ink, respectively. Re and We refer to the ratio of the inertial force to the viscous force, and the balance between the inertial force and the surface tension, respectively, while Oh relates the viscous force to the inertial force and surface tension. Generally, the Z parameter ($Z = 1/\text{Oh}$) is commonly used to indicate printability, where a Z value between 1 and 10 is expected to generate a stable drop formation.³⁹ At a low value of Z, viscous dissipation prevents drop ejection, whereas at a high value the primary drop is accompanied by a large number of satellite drops. Thus, by modulating the ink composition, inks with the desired viscosity and surface tension can be achieved to inkjet print stable droplets.

Besides generating stable droplets, for functional material based ink, it is also essential to avoid solute clogging and blockage during the printing process. Generally, the clogging issue is induced by an overlarge size of solute, solvent evaporation in an orifice and/or poor dispersion of the ink. Generally,

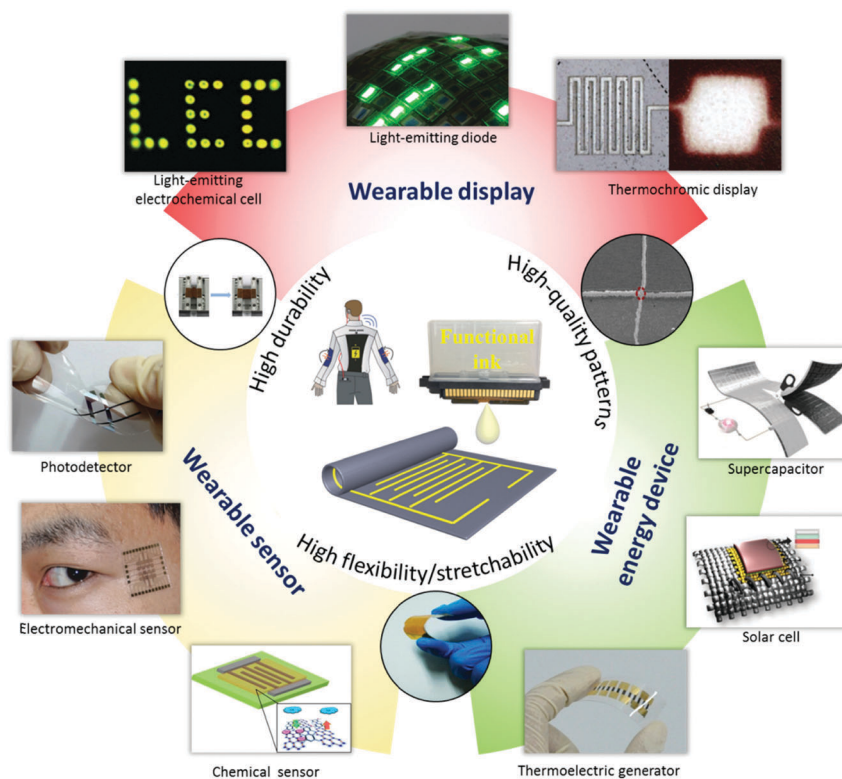


Fig. 1 Characteristic properties and diverse applications of inkjet-printed wearable electronics. "Wearable electronics on human body": reproduced with permission from ref. 24. Copyright 2013 Royal Society of Chemistry. "High-quality patterns": reproduced with permission from ref. 25. Copyright 2013 Wiley. "High flexibility/stretchability": reproduced with permission from ref. 26. Copyright 2016 Wiley. "High durability": reproduced with permission from ref. 26. Copyright 2016 Wiley. "Light-emitting electrochemical cell": reproduced with permission from ref. 27. Copyright 2014 Wiley. "Light-emitting diode": reproduced with permission from ref. 28. Copyright 2009 Nature. "Thermochromic display": reproduced with permission from ref. 29. Copyright 2009 Royal Society of Chemistry. "Photodetector": reproduced with permission from ref. 30. Copyright 2014 Elsevier. "Electromechanical sensor": reproduced with permission from ref. 31. Copyright 2015 Wiley. "Chemical sensor": reproduced with permission from ref. 32. Copyright 2016 Elsevier. "Supercapacitor": reproduced with permission from ref. 33. Copyright 2015 American Chemical Society. "Solar cell": reproduced with permission from ref. 34. Copyright 2014 Elsevier. "Thermoelectric generator": reproduced with permission from ref. 35. Copyright 2014 Royal Society.

the size of the solute should be less than 1/10th of the diameter of the printer's printhead orifice to ensure smooth printing.⁴⁰ For ink with overlarge functional materials, approaches such as the membrane filtering process and sonication-driven scission process can be adopted to obtain solutes with a suitable size.^{41,42} To avoid solvent evaporation in orifices, ink with a high boiling point is desired to keep the solvent volatility sufficiently low.⁴³ For poorly dispersed ink, agglomeration and sedimentation, which are mainly caused by van der Waals forces, are unwanted due to the possibility of clogging the inkjet nozzle. Typically, this problem could be solved by functionalizing the materials with a suitable chemical group^{44–46}/polymer coating,^{47,48} adding a surfactant^{49,50} and by introducing a good solvent.^{51,52}

2.2 Functional inks' preparation for wearable electronics

Functional materials used for inkjet printing wearable electronics can be divided into conductors, semiconductors and dielectrics according to their electrical property. Both organic and inorganic materials can be used for inkjet printing electronics. Organic materials are preferred due to their flexibility, low cost and simple synthesis, although inorganic materials often possess better electrical performance. A compromise can sometimes be

achieved by using hybrid complementary heterostructures based on organic and inorganic materials, as they may combine the desirable characteristics of both components. There is a strong demand to develop inkjet-printable inks based on high-performance electronic materials to expand the scope of possible applications for printed wearable electronics. In the following subsections, the organic and inorganic conducting, semi-conducting and dielectric materials will be discussed, with a focus on the printable materials suitable for wearable electronics. In the following, we highlight the functional-materials-based inks that are relevant to inkjet print wearable electronics, typically covering the materials and strategies to satisfy the requirements discussed above.

2.2.1 Conductor-based inks. Conductors are the most requisite constitution for all kinds of wearable electronics because of their function in building a connection between the different components of the devices. Many kinds of conducting materials, including metals, conducting polymers and other conducting organic materials (carbon-based materials), have been employed for inkjet printing wearable electronics.

Metals are intensively adopted as conductors in printing electronics due to their advantages of offering high and stable

conductivity. Metals can be printed by using inks based on metallic particles or precursors. Among these, gold (Au) demonstrates the most superior conductivity, stability and inertness as a biocompatible candidate for printed wearable electronics, and can even be utilized when in contact with living tissues.⁵³ Silver (Ag) is the most commonly used metal in printing wearable electronics because of its comparable outstanding properties, while it also still retains relatively acceptable costs.⁵⁴ Apart from these noble metals, copper (Cu), aluminium (Al) and nickel (Ni), which are easily oxidized in air due to their low oxidation potential, are also investigated because of their economic advantage. One of the solutions to the oxidation problem lies in capping the ink material with a protective layer.^{55,56} Lee *et al.* synthesized air-stable copper nanoparticles by coating a thin defective carbon shell, with which well-formulated nanoinks and conductive patterns could be realized.⁵⁷ Another approach depended on the aid of a reducing agent in the ink solvent by using electroless plating⁵⁸ or pulsed laser⁵⁹/intense light.⁶⁰ Singler *et al.* fabricated fine lines of Cu with low electrical resistivity by sequential inkjet printing of an aqueous dispersion of mussel-inspired poly(dopamine) nanoparticles and site-selective electroless plating.⁵⁸ Grigoropoulos *et al.* introduced the high-resolution direct patterning of Ni electrodes through the reductive sintering of a solution-processed NiO with the reducing agent toluene, which was initiated by laser power.⁶¹ Besides the air disability problem, to avoid clogging and to prepare a well-dispersed ink, metal nanoparticles are always capped with protecting agents. Therefore, thermal annealing is often required to achieve highly conducting patterns by removing the protecting agents and sintering the metal nanoparticles to some extent, but this prohibits their utilization on most flexible substrates for wearable electronics. Therefore efforts have been devoted to exploring annealing-free or low-temperature annealing processing. Magdassi *et al.* presented an annealing-free conductive nanoink based on a built-in sintering mechanism (Fig. 2A).⁶² By adding a destabilizing agent NaCl, which triggers detachment of the polymeric stabilizer from the surface of nanoparticles, Ag nanoparticles underwent self-sintering during the drying stage of the printed pattern spontaneously, which eliminated the need for a post-sintering process. Chun *et al.* developed a new kind of low-temperature processable Ag-salt-based conductive ink, which eliminated the need for capping with a protecting agent and also enriched the overall metallic content.⁶³ Reactive inks are also used for patterning high-conductivity features at mild temperatures.^{64,65} Other than metallic nanoparticles, metallic nanowires, such as the commonly used silver nanowires, also demonstrate huge potential in wearable electronics, such as in flexible transparent electrode manufacturing.^{17,42} The length of the nanowires should be controlled to prevent blocking of the jetting nozzles during printing.

Conducting polymers, such as poly(3,4-ethylene dioxithiophene)-poly(styrene sulfonate) (PEDOT:PSS), polypyrrole (PPy) and polyaniline (PANI), have attracted considerable interest due to their ease of processing, flexibility, lightweight, biocompatibility and the potential for low-cost device fabrication.⁶⁶ One particularly attractive feature of conducting polymers is

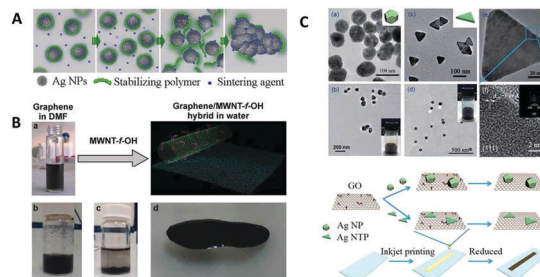


Fig. 2 (A) Schematic of the stabiliser detachment of Ag ink, which leads to the particle self-sintering process. Reproduced with permission from ref. 62. Copyright 2011 American Chemical Society. (B) The formation of a graphene/hydrophilic-functionalised MWCNT superstructure, and a well-dispersed water-based ink. Reproduced with permission from ref. 45. Copyright 2015 Wiley. (C) Up: Transmission electron microscopy (TEM) graphs of the rGO/Ag nanoparticles hybrid ink and the rGO/Ag nanotriangle platelets hybrid ink. Down: Schematic illustration of the inkjet printing of the hybrid ink for conducting patterns. Reproduced with permission from ref. 88. Copyright 2014 Royal Society of Chemistry.

that their mechanical properties are more comparable to flexible substrates, making them ideal candidates for implementation with wearable electronics. However, in comparison with metallic and carbon-based conductors, the conductivity of conducting polymers is still insufficient for many applications. In order to enhance their electric performance, strategies such as doping a high boiling solvent or surfactant have been investigated. Asawapirom *et al.* improved the conductivity of PEDOT:PSS by adding the solvents tetramethylene sulfone (TMS) and dimethyl sulfoxide (DMSO), which induced conformational changes and yielded more linear intra-chain structure and inter-chain interactions.⁶⁷ Bao *et al.* fabricated highly conductive and transparent PEDOT:PSS films by incorporating a fluorosurfactant as an additive.⁶⁸

Other conducting organic materials, including carbon-based graphene and carbon nanotubes (CNTs), exhibit a desirable combination of electrical conductivity, chemical stability and mechanical flexibility. The challenge for their application in wearable electronics as conducting inks lies in their poor dispersion in solvents owing to the strong hydrophobic character of the materials.^{69,70} With the assistance of van der Waals adsorbed surfactants or covalently attached hydrophilic groups, improved dispersion can be achieved for the solution processing method and to meet the requirement of printability.^{71–73} Coleman *et al.* presented a method to produce graphene dispersions stabilized in water by adding the surfactant sodium cholate.⁷⁴ By functionalizing single-wall carbon nanotubes (SWCNTs) with hydrophilic groups, such as carboxylic acid, amide, poly(ethylene glycol) and poly(aminobenzene sulfonic acid), Vajtai *et al.* prepared water-based stable nanotube inks, with which microscopic patterns of conducting films could be deposited by inkjet printing.⁴⁶ Zboril *et al.* provided well-dispersed graphene ink with the assistance of a hydrophilic-functionalized multiwall carbon nanotube (MWCNT) stabilizer (Fig. 2B).⁴⁵ The superstructure exhibited not only high dispersibility in water but also excellent electrical conductivity, enabling its applicability in highly conductive ink technologies. Here, the polymer or surfactant

stabilizer enhanced the ink stability and printing performance, but required an additional high-temperature post-decomposition to achieve optimal electrical properties.⁷⁵ By alternative means, a solvent exchange method, which relies on a large difference in solvent boiling points, was introduced to prepare a high-concentration and surfactant-free liquid dispersion.⁷⁶ Östling *et al.* exchanged the solvent dimethylformamide, which was used to exfoliate natural graphite flakes, by the solvent terpineol through distillation, by which method concentrated graphene ink was achieved.⁷⁷ For graphene, another approach is to alternate graphene by graphene oxide (GO), which could form a stable dispersion because of its abundance of functional groups.^{78,79} This technique usually requires a reduction process to regain the electrical performance of pristine graphene. Besides the dispersion issue, due to the high aspect ratio of CNTs, their length should be limited based on the diameter of the printhead orifice to prevent clogging.

Conducting material hybrids are also promising materials for inkjet printing wearable electronics because they combine the advantageous properties of each component to fulfil the conducting ink criteria, and sometimes even achieve performances that surpass those of the counterparts.⁸⁰ Hybrids, such as metal/conducting polymers,^{81,82} metal/carbon-based materials^{83,84} and carbon-based material/conducting polymers,^{85–87} have been investigated to hybrid the advantages of each individual component. Song *et al.* inkjet-printed highly conductive patterns with metal and graphene-based hybrid ink (Fig. 2C).⁸⁸ Hybrid GO/Ag nanocomposites combine the high electrical conductivity of Ag nanoplatelets with the enhanced mechanical compliance, electrical performance and optical transparency of the GO backbone. Furthermore, Ag nanoplatelets self-assembled on GO also serve as a dispersant and stabilizer for the ink. Neuman *et al.* formulated well-performing printing inks by combining the processability of the conductive polymer PETOT:PSS with the high conductivity of CNT.⁸⁹

2.2.2 Semiconductor-based inks. Semiconductors play prominent roles in electronic components, such as field-effect transistors. Inorganic semiconductors usually have better performance and stability, while organic semiconductors typically have superior processability and flexibility.

Typical inorganic semiconductor materials include Si, oxides of transition metals and chalcogenides. While inorganic semiconductors exhibit superior electric performance and excellent environmental stability, they often suffer from a number of drawbacks, such as inadequate dispersion and high-temperature post processing, which are incompatible for most wearable substrates.⁹⁰ Since the drawbacks of semiconductor ink are similar to those of metallic ink, it is suggested that the strategies designed for metallic ink should also be adopted here. By employing solvent exchange and polymer stabilization techniques, Östling *et al.* developed a reliable and efficient technology to effectively address critical issues associated with normal MoS₂ liquid dispersions (such as incompatible rheology, low concentration and solvent toxicity), and hence could directly and reliably write uniform patterns of high-quality MoS₂ nanosheets at a resolution of tens of micrometres.⁵¹ Dasgupta *et al.* demonstrated

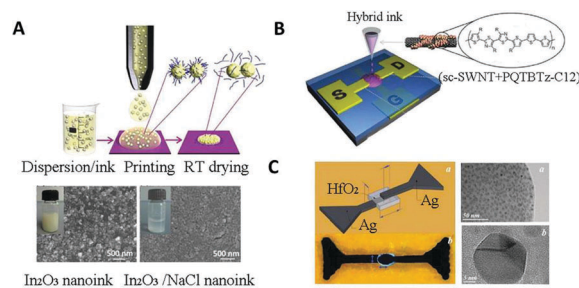


Fig. 3 (A) Up: Schematic of the chemically controlled destabilization and flocculation process of the printed nanoink droplets. The NaCl-loaded semiconducting oxide nanoinks show spontaneous stabilizer removal from the nanoparticle surface during the ink drying process. Down: Scanning electron microscopy (SEM) images of the printed surface topography with In₂O₃ nanoink and In₂O₃/NaCl nanoink. Reproduced with permission from ref. 91. Copyright 2015 American Chemical Society. (B) Schematic of a transistor built with a well-dispersed PQTBTz-C12/SWCNT nanohybrid semiconducting ink using inkjet printing. Inset: Schematic picture of the PQTBTz-C12-wrapped SWCNT. Reproduced with permission from ref. 114. Copyright 2012 American Chemical Society. (C) Left: Scheme and microscopy image of an inkjet-printed Ag/HfO₂/Ag capacitor with HfO₂ as the dielectric ink. Right: TEM images of HfO₂ thin film annealed at 250 °C for 3 h deposited on Ag bottom contact films. Reproduced with permission from ref. 116. Copyright 2016 Royal Society of Chemistry.

an approach that enabled completely room-temperature processing for the semiconductor nanoparticles n-type In₂O₃ and p-type Cu₂O through a chemically controlled curing process of the printed nanoparticle ink (Fig. 3A).⁹¹ By adding the destabilized agent NaCl, the semiconducting oxide ink showed spontaneous stabilizer removal from the nanoparticle surface during the ink drying process.

While the electric performance of organic semiconductors does not yet compare with that of inorganic semiconductors, and is limited by hopping transport between polymer chains in disordered regions, this class of materials has been touted for their ability to offer low-cost, high flexibility and enhanced processibility.^{92–94} Unlike inorganic semiconductors where a high processing temperature is required, organic semiconductors only need solvent evaporation after solution deposition. Low-temperature processing compatibility with various plastic substrates, combined with intrinsic mechanical flexibility make organic semiconductors suitable for flexible wearable electronics. The semiconductor inks for inkjet printing electronics can be prepared from polymeric organic semiconductors, such as poly[5,5'-bis(3-dodecyl-2-thienyl)-2,2'-bithiophene] (PQT-12)^{69,95} and poly(3-hexylthiophene) (P3HT),^{96,97} or small molecule organic semiconductors, such as 6,13-bis(triisopropyl-silylethynyl) pentacene (TIPS-PEN)^{98,99} or benzothieno-[3,2-*b*]benzothiophene (BTBT).¹⁰⁰ Issues with air and water sensitivity can be addressed through manipulation of the molecular structure.¹⁰¹ The solubility of organic molecules can also be adjusted by adding hydrophilic-chains to the polymer backbone or by using a soluble precursor.¹⁰²

Carbon nanotubes, which are referred to as conducting materials in Section 2.2.1, are also promising candidates as high-mobility semiconductors. One of the main obstacles to the wide usage of nanotubes in printed electronics is that they

generally show both metallic and semiconducting behaviours depending on their chirality, which is denoted by the indices (n,m) showing the wrapping direction of the graphene sheet.¹⁰³ The nanotubes show metallic property when the value of $|n - m|/3$ is an integer, otherwise they demonstrate semiconducting behaviour.¹⁰⁴ Recently, a number of methods have been developed to separate semiconducting nanotubes from metallic nanotubes, such as by density gradient centrifugation,¹⁰⁵ gel chromatography,¹⁰⁶ partition separation,¹⁰⁷ washing after growth¹⁰⁸ and sorting by conjugated polymers.¹⁰⁹ Taking sorting by conjugated polymers as an example, Bao *et al.* employed several kinds of solvents for the sorting of semiconducting SWCNTs by poly(3-dodecylthiophene) (P3DDT). The dispersion yield could be increased to over 40% using decalin or *o*-xylene as the solvent while maintaining high selectivity to semiconducting SWCNTs.¹¹⁰

Semiconducting hybrids are also being investigated because they combine the advantages of each part and yield properties that are not available in a single-component system. Semiconducting hybrids, such as organic semiconductor/carbon-based semiconductors¹¹¹ and inorganic semiconductor/organic semiconductors,^{112,113} have shown enhanced charge carrier mobility with high flexibility and enhanced processibility. Kim *et al.* hybridized the polymer semiconductor poly(didodecylquaterthiophene-*alt*-didodecylbithiazole) (PQBTz-C12) and SWCNTs to achieve improved electrical property, based on which a high-performance inkjet-printed TFT was fabricated (Fig. 3B).¹¹⁴ This is due to that the SWCNTs can improve the molecular order and modulate the interaction of the semiconducting polymers.

2.2.3 Dielectric-based inks. Electrical insulating materials with high capacitance are necessary in electronic devices, such as transistors and capacitors, for preventing shortages from crossing conducting wires. Printable dielectric materials used for wearable electronics include inorganic materials, polymers and organic/inorganic hybrid dielectrics.¹¹⁵ Inorganic dielectrics, such as silica (SiO₂) and alumina (Al₂O₃) often require high-temperature processing due to the need for annealing for high-density films with low leakage current and due to the decomposition of the organic compounds used to enhance dispersion. Among these, metal-oxide dielectrics with a high dielectric constant (k) have drawn considerable attention due to their high dielectric constant. Vescio *et al.* demonstrated a fully-printed metal-dielectric-metal capacitor with high homogeneity and good integrity on a flexible substrate, where the high- k hafnium oxide (HfO₂) was selected as the dielectric (Fig. 3C).¹¹⁶ Organic dielectric materials are highly desirable due to the low-temperature processing, high dielectric strength and high flexibility. Some of the commonly used insulating polymers in electronic applications are poly(4-vinylphenol) (PVP), poly(methyl methacrylate) (PMMA), polyethylene terephthalate (PET), polyimide (PI), polypropylene (PP), polyvinyl alcohol (PVA) and polystyrene (PS). Hybrid structures, such as high- k metal-oxide-embedded polymer dielectrics, show an enhanced dielectric constant and leakage current. Highly stable dielectric properties that can endure a strained environment are ultimately required for employment in flexible and stretchable applications.

3. Strategies to inkjet print high-performance wearable electronics

To inkjet print wearable electronics with high performance, there are several key considerations required, including the pattern quality, device flexibility/stretchability and device durability. A high-quality pattern is a prerequisite for device construction, since a uniform and high-resolution pattern enhances the device stability and can help minimize the device size. Large flexibility/stretchability and long durability ensure the device is adaptable for wearable applications. In this section, we present a brief introduction to the strategies to meet the requirements for good device performance.

3.1 Strategies to achieve high-quality patterns

Advanced and flexible wearable electronic devices demand uniform and high-resolution patterning techniques for high performance and small size. Uniform patterns ensure the homogeneity and stability of the device properties. For instance, they diminish situations such as heterogeneous conductivity and short circuits of the printed circuit. High-resolution patterns enable the use of a smaller area of the electronic board, which provides convenience for wearable electronics. Besides size minimization, they also improve device performance, such as a higher density and conductivity for circuits and a larger bandwidth and higher switching speed for transistors.¹⁶

Serving as a basic constitution of printed patterns, uniform and high-resolution dots and lines are highly required. Since high-resolution depositing dots have been reviewed by Song's group previously,^{11,12} in this section we only discuss printed lines, which in fact are more intensively used. Unlike separate dots, lines are prepared by inkjet printing consecutive droplets. The droplet-surface interaction and the drying dynamics of the droplets dominate the final shape of the printed structure. In order to achieve patterned lines meeting the desired requirements, a well-behaved coalescence process and controlled drying procedure are required. Herein, we discuss strategies to obtain uniform and high-resolution lines in view of controlling the liquid footprint and solute deposit.

3.1.1 Inkjet printing of patterns with high uniformity. The coalescence of consecutive droplets in a straight line without waving or bulging disability ensures the uniformity of printed patterns. Investigations into consecutive droplets coalescence start with the dynamics of two droplets coming into contact with each other.¹¹⁷⁻¹¹⁹ The process of droplet coalescence (Fig. 4A) can be distinguished into three physical stages: (i) rapid healing of the bridge between the drops, (ii) a slower rearrangement of the liquids and (iii) a mixing of the fluids. Particles' movement and deposition inside the liquid are in accordance with the droplet behaviour.¹²⁰ In the coalescence process, the drop space and delay time play predominant roles in determining the deposition morphology, as shown in Fig. 4B.¹²¹ Varying the droplet distance can directly achieve an inkjet-printed line with morphologies of individual, scalloped, uniform, bulging and stacked coins. Besides the drop space, it should also meet the prerequisite of a suitable delay time between the neighbouring droplets to

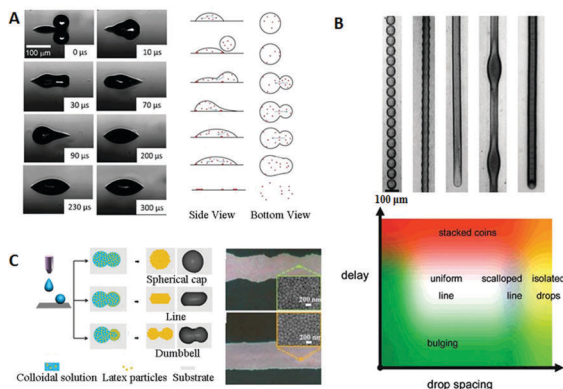


Fig. 4 (A) Left: Side-view images for the impact and coalescence of two consecutively printed drops. Right: Schematic of the drop impact, coalescence, carrier liquid evaporation, and particle deposition of two consecutively printed evaporating colloidal drops. Reproduced with permission from ref. 120. Copyright 2012 Royal Society of Chemistry. (B) Up: Principal printed line behaviours with the decrease of drop spacing, namely: individual drops, scalloped, uniform, bulging and stacked coins, respectively. Down: The effect of drop spacing and time delay on the behaviour of a printed line at an intermediate temperature. Reproduced with permission from ref. 121. Copyright 2008 American Chemical Society. (C) Left: Three typical coalescing cases of the neighbouring ink droplets induced by different dynamic wettabilities of ink droplets on the substrates. They form spherical cap, line and dumbbell structures, respectively. Right: Optical microscope images of the as-printed silver lines with wave and straight footprints. Reproduced with permission from ref. 122. Copyright 2014 American Chemical Society.

prevent the drops from coalescing into a larger one or keeping them as isolated drops. Since the surface tension and solute concentration of a bi-solvent based ink change along with the drying process, Song *et al.* investigated the effect of the dynamic wettability on the final morphology of a line, which consisted of spherical caps, straight lines and dumbbells (Fig. 4C).¹²² The droplets coalescence of liquids with different viscosities,¹²³ densities¹²⁴ and volumes¹²⁵ was also studied for a further understanding of droplet behaviour, which could lay a foundation for inkjet printing straight lines of different materials.

3.1.2 Inkjet printing of patterns with high resolution. In order to achieve patterns with high resolution, which thereby would increase the integration degree and electrical stability of the printed electronics, strategies should be devoted to increase the footprint resolution or to modulate the solute depositing behaviour. Increasing the footprint resolution provides primary approaches by reducing the depositing area of printed lines, while modulating the solute depositing behaviour focuses on the rearrangement of the functional materials in the ink during the drying process.

3.1.2.1 Increasing the footprint resolution. For the purpose of increasing the footprint resolution, several strategies have been developed, including: (i) modulating the ink spreading and retracting behaviours on substrates, (ii) adjusting the printing parameters and (iii) exploring novel apparatus. By increasing the footprint resolution, the distances between dots or lines are also able to be minimized, which further diminishes the integration density.

As is known, the property of the substrate governs the spreading and retracting behaviours of the printed droplets on a substrate, which further determines their final size. One approach therefore is to modify the wettability of the substrate, such as decreasing the surface tension and increasing the roughness. Whitesides *et al.* modified a substrate with a low surface energy coating to enlarge the contact angle of the ink droplet, thus minimizing the spreading degree and footprint size of the resulting patterns (Fig. 5A).¹²⁶ A fluorine-treated polyimide film with a porous structure was used by Nogi *et al.* to further restrict the spreading of the ink.¹²⁷ Another approach is to adopt substrates with a prepatterned physical/chemical structure. Unlike those substrates on which ink spreads spontaneously, endowing the substrate with a prepatterned substrate provides an efficient approach to force the ink to remain in a preferred area,^{128–130} thus resulting in an improved printing resolution.^{131–135} Frisbie *et al.* fabricated highly conductive wires with high-resolution and a minimum line width of 2 μm by inkjet printing a reactive Ag ink into physical patterned channels that were fabricated by imprint lithography (Fig. 5B).¹³² Lam *et al.* improved the resolution and accuracy of printed PEDOT:PSS conductive patterns by employing a chemical hydrophilic–hydrophobic patterned surface. They found the high wettability contrast between the hydrophilic area and the hydrophobic area provided a huge surface energy barrier to restrict the droplet spreading.¹³⁵ Besides these solid substrates whose morphology remains unchanged during the printing process, a viscoelastic liquid surface has also been an alternate for preparing high-resolution patterns.¹³⁶ Here, when an inkjet droplet impacts on the viscoelastic liquid substrate, the ink would be wrapped by the surface, which consequently leads to its retraction.^{137,138} Song *et al.* found that high-resolution microgrooves with a width of 8.7 μm could be fabricated by inkjet printing on a procured polydimethylsiloxane (PDMS) substrate, depending on the deformation and detracting mechanism (Fig. 5C).¹³⁹ Ag nanoparticles were then patterned into the microgrooves and subsequently transfer-printed onto PET surfaces for high-resolution conductive wires.

Besides the use of particular substrates for a more confined liquid spreading behaviour, the inkjet-printing parameters also affect the liquid footprint size.^{140,141} For instance, a decrease in line width is observed when the dot spacing increases.¹⁴² A stable line width has been shown to be bounded by two limits, with the lower bound (minimum line width) determined by the maximum drop spacing for stable coalescence and the upper bound (maximum line width) determined by the minimum drop spacing below which a bulging instability occurs.

Intuitively, another obvious way to minimize the footprint size of dots or lines is to reduce the nozzle diameter. However, droplets are difficult to be generated and ejected from a nozzle with a sub-micrometre diameter due to the large resisting capillary pressure at the ejection opening. However, special printing apparatus has been developed to overcome these limitations and to print high-resolution patterns. The use of an electrohydrodynamic jet that applies an electric field to create the fluid flows for ejecting and depositing inks onto a substrate provides a way to inkjet ultra-small droplets because of the Taylor cone

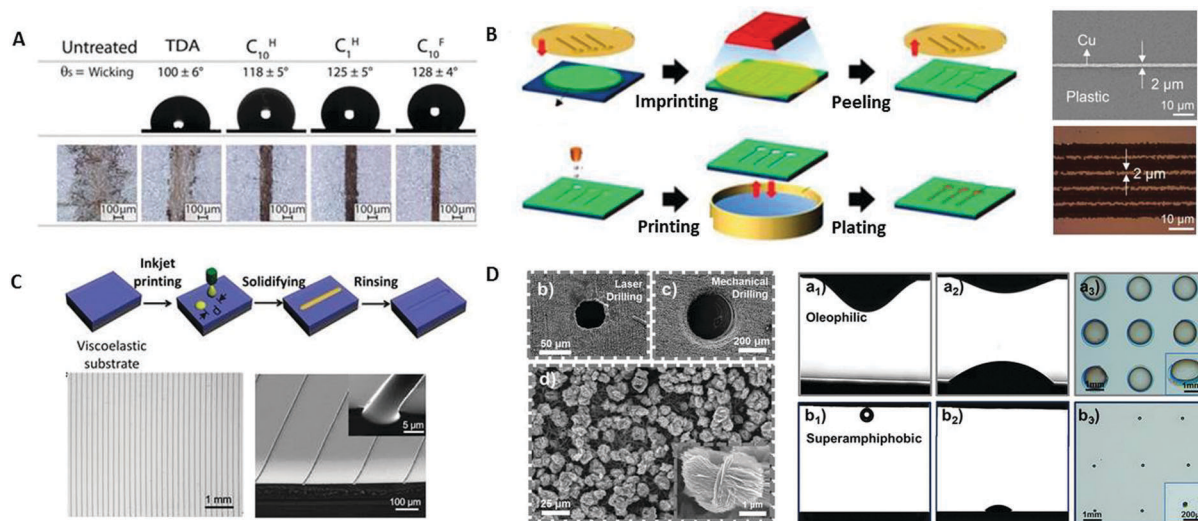


Fig. 5 (A) Up: Images of 10 μL drops of water on a series of Canson tracing papers, modified with different organosilanes, and their corresponding static contact angles. Down: Optical micrographs of silver wires printed on modified or unmodified Canson tracing paper substrates using the reactive silver ink, showing that the substrate high surface energy could minimize the spreading degree and footprint size of the resulting patterns. Reproduced with permission from ref. 126. Copyright 2014 Wiley. (B) Left: Schematic illustration of the prepatterned substrate-assisted inkjet printing process. By inkjet printing a reactive Ag ink into physical patterned channels fabricated by imprint lithography, high-resolution conductive wires are achieved. Right: SEM images and optical micrographs of the inkjet patterning of high-resolution conductive wires. Reproduced with permission from ref. 132. Copyright 2015 American Chemical Society. (C) Up: Schematic of the inkjet-imprinting processes. By inkjet printing poly acrylic acid ink onto the precured viscoelastic PDMS surfaces, high-resolution patterns are achieved. Down: Optical image and SEM images of the printed microgroove patterns. Reproduced with permission from ref. 139. Copyright 2015 Wiley. (D) Left: Morphology characterization of the superamphiphobic nozzle surface. Right: Optical images of oil droplets dispensed from a nozzle surface, and stereo microscope image of the final pattern after solvent evaporation by using a nozzle and superamphiphobic nozzle, respectively, showing an increased resolution in inkjet printing by the superamphiphobic nozzle. Reproduced with permission from ref. 147. Copyright 2015 Wiley.

formed at the tip of the capillary.^{143,144} Rogers *et al.* achieved sub-micrometre resolutions with a minimum diameter of 240 ± 50 nm by electrohydrodynamic-jetting inks from a fine capillary nozzle with a diameter of 300 nm.¹⁴⁵ Efforts have also been made to modify the wettability property of the nozzle.¹⁴⁶ Song *et al.* presented a superamphiphobic nozzle for producing tiny droplets down to the picolitre scale without using any extra driving forces (Fig. 5D),¹⁴⁷ which represents a method that could be potentially applied to commercial inkjet nozzles to overcome the hampering pressure.

3.1.2.2 Modulating the solute depositing behaviour. Another method to increase the printing resolution and device integration density is to modulate the depositing behaviour of the solute. By changing the ink constitution,^{148–152} the substrate property^{153,154} and the drying atmosphere,^{155,156} the inward Marangoni flow,¹⁵⁷ outward capillary flow¹⁵⁸ and the three-phase contact line (TCL) sliding behaviours can be altered, which leads to a different solute depositing distribution.

Many researchers have made efforts to concentrate solutes in the centre of the droplets. By adopting ellipsoidal particles,¹⁴⁸ increasing the droplet viscosity¹⁵⁹ and regulating the droplet pH value,¹⁵² the outward capillary flow will be suppressed, which prevents solutes from continuously moving to the periphery of the droplets. Adding ink with a higher boiling point and lower surface tension solvent¹⁵¹ or adding ink with a surfactant¹⁵⁰ that contributes to an increased inward Marangoni flow can result in

more solutes gathering in the centre of the droplet. It is to be noted that these methods exert more impact on modulating the solutes distribution than on increasing the final depositing resolution when the drying process takes place on a substrate where the droplet TCL tends to pin. Different from the highly-adhesive substrates, an enhanced resolution is achieved when the drying process takes place on a substrate where the droplet TCL slides inward. Song *et al.* inkjet-printed a close-packed pattern sized 1.6 μm from a 25 μm orifice on a substrate with a high receding contact angle based on the depinning mechanism (Fig. 6A).¹⁵⁴

Contrary to those approaches trying to increase the inward flow of the solutes, efforts have also been devoted to boosting the solutes' outward flow to the maximum extent to achieve high resolution printing.^{58,160–162} Song *et al.* inkjet-printed a series of conductive silver patterns with an average width of 5–10 μm by utilizing the coffee-ring effect (Fig. 6B).¹⁵³ They controlled the particle migration within the evaporating droplets by adopting hydrophilic substrates, upon which an increased outward capillary flow carried the suspended silver nanoparticles to the contact line, resulting in two assembled parallel lines.

3.2 Strategies to achieve high flexibility/stretchability

Wearable electronics, including electronic accessories, electric clothes and electric skin, tend to be bent or stretched during usage. Thus, flexibility and stretchability are primary mechanical considerations when it comes to inkjet printing wearable electronics.

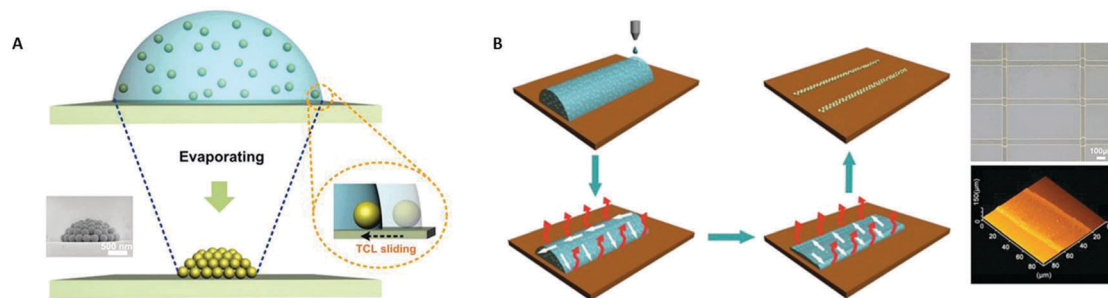


Fig. 6 (A) Schematic of the sliding TCL reversing coffee-ring effect on a low-adhesive substrate. The inset SEM image is the printed dome with a diameter of 1.6 μm . Reproduced with permission from ref. 154. Copyright 2014 Wiley. (B) Left: Schematic of inkjet printing silver nanoparticles patterns induced by the coffee-ring effect. Right: Optical image and atomic force microscope (AFM) image of reticular silver patterns fabricated by the coffee-ring effect. Reproduced with permission from ref. 153. Copyright 2013 Wiley.

To meet the requirements, strategies such as exploring more suitable substrates or patterns are investigated.

3.2.1 Inkjet printing flexible wearable electronics. To inkjet print flexible devices, the specific properties of inks and substrates are crucial factors to take into consideration, whereby utilizing appropriate flexible substrates is particularly important and fundamental. Instead of conventional rigid substrates, flexible substrates, such as plastics, papers, textiles and elastomers, can be adopted to inkjet print wearable electronics. The mechanical properties determine the substrate's application purposes. Plastic and paper substrates are more used in electronic accessories due to their inherent excellent flexibility despite their poor stretchability. Plastics are more used in long-lasting applications, while papers tend to be applied for disposable situations. For clothes-based electronics, textiles are the primary choice due to their softness and high porosity, which means they are able to wrap comfortably around curvilinear human skins with millions of pores to allow the skin to breathe. Elastomers remain the best choice for electronic skins on account of their remarkable flexibility and stretchability. Note, due to the stretchable nature of elastomers, they will be discussed in the "Strategies to inkjet stretchable wearable electronics" section. For these flexible substrates, problems such as overspreading and an incompatible high temperature may be encountered during the inkjet-printing process due to the typical surface properties (high porosity, roughness, hygroscopicity) and allowable temperatures of different substrates. In this section, strategies to inkjet print flexible wearable electronics will be discussed, with an emphasis on solving the encountered problems.

3.2.1.1 Plastic-based wearable electronics. Plastics are most commonly adopted as flexible substrates for inkjet-printed wearable electronics that can be applied for portable devices. The intrinsic attributes, such as the condensing and hydrophobic surface and high mechanical strength, of plastics ensure their good printing behaviours. However, since the glass-transition temperature of flexible plastic substrates is much lower than that of rigid substrates, the processing temperature must be considered when it comes to the materials need for post sintering. For example, polyimide (PI) has a glass-transition temperature (T_g)

between 360 $^{\circ}\text{C}$ and 410 $^{\circ}\text{C}$. Other polymer substrates, such as PET, polycarbonate (PC), polyethersulfone (PES), poly(ethylene naphthalate) (PEN) and polyetheretherketone (PEEK), have T_g values even lower than that. Thus for flexible plastic substrates, it is essential to develop strategies for low-temperature processing. Apart from exploring novel inks, which were discussed in Section 2.2, such as self-sinter inks,⁶² sinter-free inks⁶³ and reactive inks,^{64,65} particular low-temperature post-processing methods are also under investigation, including photonic sintering,¹⁶³ microwave sintering,¹⁶⁴ plasma sintering^{165,166} and electrical sintering.^{167,168} It is to be noted that these methods can also be applied to other substrates that cannot endure high-temperature processing.

3.2.1.2 Paper-based wearable electronics. Paper substrates offer many advantages for printed flexible electronic devices. Not only is paper widely available and inexpensive, it is also lightweight, biodegradable and can be rolled or folded into 3D configurations.^{169,170} By virtue of the abundance and physical properties of cellulose, paper-based devices are often considered to be novel platforms for inexpensive, portable and simple devices. In spite of the attractive attributes, some drawbacks are encountered when paper serves as substrate during the inkjet-printing process, such as overspreading and high-temperature post processing.

Inkjet-printing-adapted low-viscosity inks tend to be absorbed by paper substrates due to its rough and porous nature, which leads to spreading forms with wavy boundaries and an inadequate electrical property. To provide a barrier and to prevent ink dropping into these comparatively large cavities of paper, strategies that convert hydrophilic paper to hydrophobic paper are typically adopted. Various paper textures, compositions and coatings can be exploited to prevent inks from overspreading, such as employing photopaper,^{171,172} modifying papers with hydrophobic organosilanes,¹²⁶ lowering the surface roughness^{173,174} and pre-coating a smoothing underlayer.^{175,176} Photopaper, commonly used as inkjet paper, provides a packed hydrophobic surface and prevents ink permeation and overspreading.^{171,172} As a more cost-saving hydrophobic-treated paper, omniphobic "fluoroalkylated paper" has been fabricated to inkjet print electronics with a more controlled morphology.¹²⁶ Nanopaper composed of densely

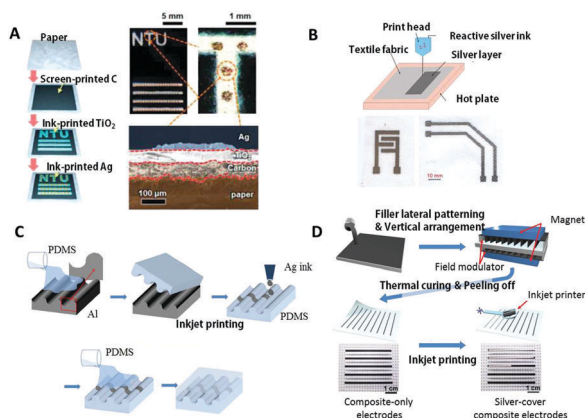


Fig. 7 (A) Left: Scheme of inkjet printing memory devices on a paper substrate, which is coated with carbon paste, *via* screen printing to achieve both a smooth layer and bottom electrode. Down: Photograph, optical image and cross-sectional SEM image of the paper-based memory. Reproduced with permission from ref. 175. Copyright 2014 American Chemical Society. (B) Up: Scheme of inkjet printing the reactive silver ink on textile using the modified Tollens' process to ensure a low-temperature sintering fabrication. Down: Photo images of inkjet-printed silver electrodes on textiles. Reproduced with permission from ref. 183. Copyright 2016 Elsevier. (C) Scheme of fabricating high performance and stable stretchable silver electrodes by inkjet printing on a wave structured elastomeric substrate. Reproduced with permission from ref. 190. Copyright 2011 American Institute of Physics. (D) Scheme of the fabrication process of inkjet-printed stretchable electrodes by fully utilizing the unique property of negative strain-dependency in the electrical resistance of the magnetically patterned and arranged nickel composite. Reproduced with permission from ref. 193. Copyright 2014 Wiley.

packed cellulose nanofibres, which exhibits a low surface roughness and nanoporous network structure, was designed to help the ink vehicles to permeate through the nanopores and also to aid absorption along the fibril direction parallel to the surface while retaining the silver nanoparticles on the surface.^{173,174} Precoating a smoothing underlayer prevents ink from permeating and allows the paper to retain its desirable mechanical characteristics.¹⁷⁶ He *et al.* coated a paper substrate with carbon paste *via* screen printing to achieve both a smooth layer and a bottom electrode. On the precoated carbon layer, an active layer of TiO₂ nanoparticles and top electrode Ag nanoparticles were inkjet-printed successively to fabricate a flexible memory device (Fig. 7A).¹⁷⁵

Moreover, in order to use paper as a substrate in flexible electronic devices, the development of a low-temperature process (≤ 150 °C) is essential because paper is easily degraded or burnt at high temperature.¹⁷⁷ To satisfy the temperature requirement, unique ink and post-treatment, as discussed in Sections 2.1 and 4.1.1, can be adopted.

3.2.1.3 Textile-based wearable electronics. As a flexible, lightweight, long-lasting and conformable platform that can be mechanically stretched, twisted, bent or sheared, fibre-assembled textiles are promising candidates for flexible clothes-based wearable electronics.⁵ Materials such as Ag nanoparticles, SWCNT/RuO₂ nanowires and CNT/PEDOT:PSS have been inkjet-printed onto textile substrates for super-flexible wearable electronics,

such as antennas,¹⁷⁸ supercapacitors¹⁷⁹ and electroluminescent devices.^{180,181} However, to date, there have been only limited reports on the inkjet printing of textile-based electronic devices due to the inherent technical challenges of inkjet printing onto fabric substrates, namely that it is difficult to achieve a highly conductive continuous track on the rough fabric with a thin inkjet-printed layer and also as the majority of fabrics cannot withstand long-term curing temperatures above 150 °C. Thus, it is suggested to resort to solutions that have arisen for paper-based substrates, since fabric substrates share almost the same technique problems as paper-based substrates, except that the porosity of textiles is larger. Tudor *et al.* created a more uniform surface for the subsequent printing on fabrics by pre-treating them with an intermediate screen-printed interface layer, which overcome the porous problem of the textile substrate.¹⁸² Stempien *et al.* used the modified Tollens' process for the preparation of a suitable water-soluble ink containing silver to inkjet print on textile substrates for textronic applications (Fig. 7B).¹⁸³ The choice of this type of ink ensured the inkjet-printability of textile surfaces with simultaneous sintering at a low temperature not exceeding 90 °C.

3.2.2 Inkjet printing of stretchable wearable electronics. In addition to flexibility, stretchability is also highly required for wearable devices to cover arbitrary surfaces and movable parts, especially when it comes to the inkjet printing of skin-mounted electronics.^{184–187} Furthermore, electronic devices on stretchable substrates can be protected from mechanical deformation by allowing the stretchable electronics to undergo most of the mechanical stress. Among the stretchability improvement strategies, the most basic and prevalent approach involves the use of elastomer substrates during the inkjet printing. PDMS, which remains the best choice of stretchable elastomer on account of its remarkable flexibility and high thermal and chemical resistance, has overwhelmingly been used for the inkjet printing of E-skin and other stretchable electronics; albeit, other substrates may be advantageous in particular applications; for example, butyl rubber with an intrinsically low gas permeability is compatible with applications where an encapsulating barrier is needed to prevent the atmospheric degradation of sensitive electronic materials.¹⁸⁸ To further increase the stretchability, composite elastomers embedding conductive fillers are often applied. Someya *et al.* manufactured printable elastic conductors comprising SWCNTs uniformly dispersed in a fluorinated rubber using an ionic liquid and jet-milling, by which method a stretchability of more than 100% was obtained.²⁸

Since high stretchability will inevitably lead to pattern cracks, which is detrimental to the device's electric performance, it is imperative to develop strategies to inkjet print stretchable devices that still maintain their performance. Currently inkjet-printed stretchable electronics are mostly concerned about conductive circuits, thus solutions will be discussed in the view of maintaining conductivity while increasing the stretchability, which include employing one-dimensional (1D) flexible materials as inks, utilizing elastomeric substrates with a particular morphology, using composite elastomers embedding conductive fillers as substrates and applying an external constitution

(additional treatment) to the devices. Hong *et al.* inkjet-printed flexible 1D SWCNT thin films on stretchable substrates with a nitric acid post-treatment, which maintained their conductive properties under 100% tensile strain.¹⁸⁹ Hong *et al.* also developed high performance and stable stretchable silver electrodes by inkjet printing on wave-structured elastomeric substrates¹⁹⁰ and pre-stretched elastomeric substrates (Fig. 7C).¹⁹¹ Jeong *et al.* designed electric circuits directly onto an electrospun fibre mat by inkjet printing using the Ag nanoparticle precursor solution.¹⁹² Ag nanoparticles could be found in the interior and on the surface of the fibres, both of which provided electron pathways and contributed to preserving the conductivity of the circuit under large deformations. Hong *et al.* developed a highly stretchable electrode and demonstrated a resolution sustaining lighting device by fully utilizing the unique property of negative strain-dependency in the electrical resistance of the magnetically patterned and arranged nickel composite (Fig. 7D).¹⁹³ The exposed silver-covered composite electrode kept its conductivity even up to 100% tensile strain. Other strategies to improve the stretchability of electronics while maintaining the electrical performance include patterning in deterministic fractal motifs, such as printing serpentine structures on stretchable PDMS.¹⁹⁴

3.3 Strategies to achieve high mechanical durability

Another important consideration for the inkjet printing of wearable electronics is the mechanical durability, since these portable or skin-mountable devices should be accommodated by very large, complex and dynamic strains. Dynamic durability represents the endurance of a stable electrical functionality and mechanical integrity under long-term bending or stretching movements, such as when contacted with the human skin or washed in liquid. Degradation of the performance of flexible wearable electronics mainly includes cracking and slipping. The mechanisms of mechanical failure and strategies to achieve remarkable dynamic durability are discussed below.

3.3.1 Minimizing device cracks. Cracks are usually generated during the fabrication process and applying process. During inkjet printing and the post-sintering process, cracks arise from solvent evaporation and the thermal expansion coefficient difference between the electronic pattern and substrate, which are overcome in part through the deposition of thicker tracks.¹⁹⁵ When it comes to device durability, it is necessary to minimize cracks generated during usage. Researchers usually observe device cracks fatigue resistance in bending/unbending or stretching/releasing tests. Cracks happen once the maximum tensile stress reaches a critical tensile stress upon bending and stretching movements. Cracks originate at the stress concentrated areas, which are initially typically small and negligible, but then propagate until the mechanical performance of a part is severely impaired. The generation of cracks critically limits the electrical performance of devices. Crack-free devices call for good flexibility and resilience, with minimal degradation in the electrical performance after thousands of bending cycles. It is essential to diminish the cracks in printed wearable electronics, which is realized by increasing the critical tensile stress or decreasing the tensile stress applied on the device.

By applying mechanical flexible inks or substrates, the origination and propagation of cracks are more prone to be prohibited during usage under dynamic loading, ensuring the durability of the devices. Typically, functional materials in ink with a relatively high aspect ratio and which are confined to the printability size window can be adopted to reduce crack generation due to their role in producing linkages inside the device. Moreover, a suitable binder, such as hydroxyethyl cellulose, can be added to the ink to bind the functional materials together and to prevent the generation of cracks.¹⁹⁶ These approaches contribute to an enhanced critical tensile stress and consequently a reduced likelihood of cracks in devices.

Reducing the tensile strength provides another route for diminishing the cracks. Zheng *et al.* achieved flexible, foldable and stretchable metal conductors with reduced cracks and improved performance by laminating another layer of PET on top of a printed Cu layer pattern, which formed a PET/Cu/PET sandwich structure that could effectively shift the stress-neutralization plane into the Cu layer. As a result, the film stress in the Cu layer was converted from tensile stress to shear stress, which consequently reduced the cracks.¹⁹⁴ Another method to achieve an ultrahigh bending ability with reduced cracks is to utilize a thinner substrate. Zheng *et al.* discovered that by replacing the thick PET substrate with a thin PI substrate, the resistance of the printed Cu/PI sample was more stable upon bending due to the minimized tensile stress in the Cu layer.¹⁹⁴ Employing a thinner pattern could also contribute to optimization of the crack-free morphology and an outstanding bending performance.¹⁹⁷

Apart from decreasing the tendency to form cracks during bending and stretching of the device, self-healing cracks afterwards also provide a possibility to deal with the crack problem. Katz *et al.* inkjet-printed organic field transistors with pronounced electrical and mechanical self-healing behaviour by integrating a poly(2-hydroxypropyl methacrylate) (PHPMA)/poly(ethyleneimine) (PEI) self-healing polymer as a gate dielectric material (Fig. 8A).¹⁹⁸ The system exhibited pronounced self-healing behaviour on both mechanical and electrical aspects. More importantly, it could even restore the conductivity of materials coated above it simultaneously, without the need for any healing agent to be added.

3.3.2 Minimizing device slipping. Slips and delamination happen when the adhesion between the printed structures and the underlying substrates is inadequate. In printed flexible devices, adhesion is critical for the devices' stability and reliability. Researchers usually determine device slips fatigue resistance by the cross scotch tape test.¹⁹⁸ The slip between the active film and the underlying substrate layer happens when the maximum shear stress reaches the critical shear strength. Endeavours have been devoted to two aspects to solve this issue: increasing the critical shear stress for enhanced sheer resistance ability and decreasing the sheer force.

By applying a substrate with increased surface tension or by adopting a reactive interface, an increased slip resistance performance can be achieved. A thin film with a higher surface energy has a stronger tendency to be attracted to another surface,

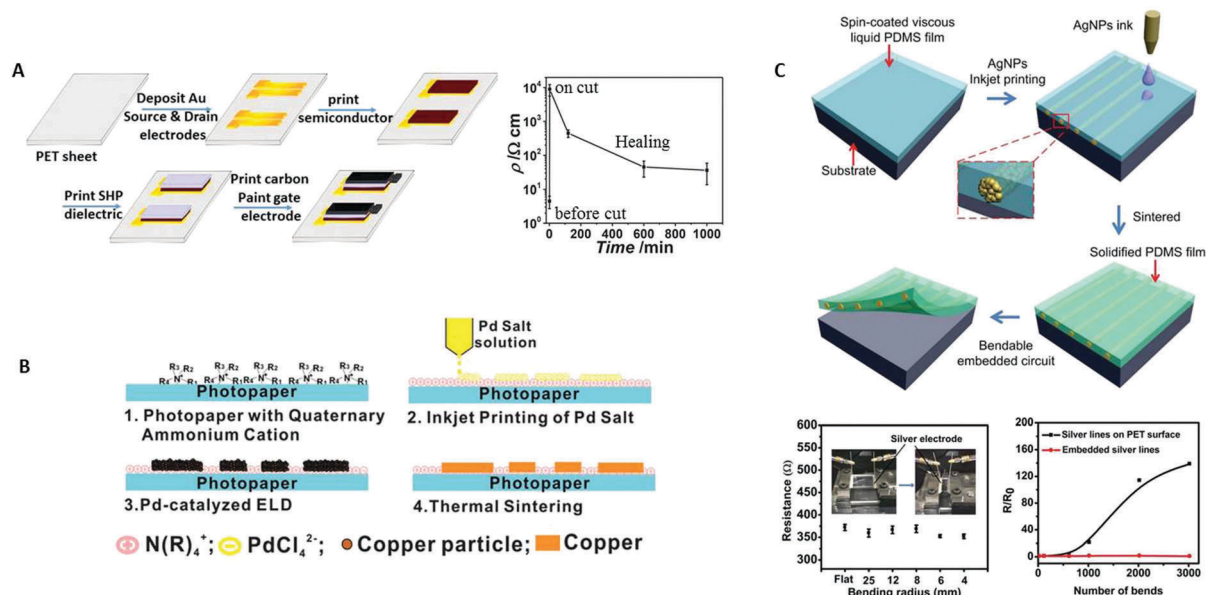


Fig. 8 (A) Left: Scheme of self-healing inkjet-printed device fabrication procedures. Right: The carbon paint (coated on a self-healing polymer) conductivity healing test, which shows long durability. Reproduced with permission from ref. 198. Copyright 2015 Wiley. (B) Schematic of preparing copper patterns with strong adhesion by the inkjet printing of a palladium salt solution with a negatively charged tetrachloropalladate group ($-PdCl_4^{2-}$), followed by electroless deposition of copper. Reproduced with permission from ref. 172. Copyright 2014 Royal Society of Chemistry. (C) Up: Schematic of fabricating fully embedded silver microcables with high adhesion and durability by inkjet printing Ag nanoparticle ink into a viscous liquid PDMS precursor film. Down: The conductivity stability test of the embedded silver microcables under different bending radii and bending numbers. Reproduced with permission from ref. 201. Copyright 2016 Wiley.

which results in a higher adhesive force between deposited patterns and substrates. Deen *et al.* exhibited printed Pd films with a high affinity and good adhesion to air-plasma-treated PI substrates.¹⁹⁹ Chiolerio *et al.* improved the adhesion of printed PEDOT:PSS ink drops to a copper-particles-embedded PDMS substrate by pre-treating the substrate in an atmospheric pressure plasma system, which was optimized by analysing a microscope image and by numerical interpretation of the printed bulging and spread.²⁰⁰ Yang *et al.* prepared copper patterns with strong adhesion to flexible photopaper by the inkjet printing of a palladium salt solution with a negatively charged tetrachloropalladate group ($-PdCl_4^{2-}$) onto the photopaper substrate with a positively charged quaternary amine group (NR_4^+), followed by the electroless deposition of copper (Fig. 8B).¹⁷² A bivalent tetrachloropalladate group combined with two monovalent quaternary amine groups when the ink droplet was in contact with the photopaper substrate, which resulted in a strong adhesion between the palladium ions and the substrate. The use of an encapsulation layer to protect the printed tracks can also be adopted to enhance the pattern adhesion to the substrate. Frisbie *et al.* fabricated Cu/Ag wires embedded in a plastic substrate, which displayed exceptional adhesion to a moulded epoxy substrate and remained anchored to the channels even after consecutive tests.¹³² Song *et al.* fabricated fully embedded silver microcables by inkjet printing Ag nanoparticle ink into a viscous liquid PDMS precursor film. As the silver cables were encapsulated in the PDMS matrix, the embedded circuits could be bent reversely without an apparent resistance increase, which thus could provide a promising

avenue to inkjet print integrated circuit boards with high adhesion and durability (Fig. 8C).²⁰¹ Moreover, inkjet printing electrical tracks into patterned substrate or viscoelastic substrate for an embedded encapsulation layer not only leads to higher mechanical durability but also raises the corrosion resistance.

The stress in thin films promotes their delamination, which can be quantitated by measuring the strain energy release rate (G). By decreasing the maximum shear stress applied to the device, the odds of slipping and delamination are decreased, which allow for a more durable device. The strain energy release rate is proportional to the film thickness (h) according to $G = Z\sigma_f^2 h/E_f$,²⁰² where Z is a dimensionless cracking parameter, σ_f is the stress in the film and E_f is the modulus of elasticity. Thus, a thinner film has a smaller strain energy release rate, indicating that it is more difficult for the film to delaminate from the substrate.

4. Applications

Serving as a rapid, precise and reproducible deposition and patterning approach, inkjet-printing technology has been employed for the large-scale manufacturing of wearable devices. Inkjet printing endows such devices with accurate multiple structures, a small feature size and high volume production. In this section, several types of wearable electronics fabricated by inkjet printing, including displays, sensors, energy devices and other devices, are highlighted and reviewed.

4.1 Wearable displays

Flexible and stretchable displays and solid-state lighting systems are now gaining widespread attention for mobile electronic devices, in which they could enable the development of expandable and foldable screens for smartphones, electronic clothing and rollable or collapsible wallpaper-like display boards. Inkjet-printing techniques have emerged as an attractive deposition technique for optoelectronic applications, which deposit inks on defined surface areas, in a desired shape. To inkjet print a wearable display, it is crucial to fabricate devices with uniform thicknesses in each layer, which directly affects the brightness and colour uniformity, because non-uniformity may lead to a localized, high electric current, localized overheating and the gradual destruction of the device.

Among the display equipment, light-emitting diodes (LEDs) are emerging as the most suitable solid-state light emitting optoelectronic devices for extensive applications, such as in multi-colour electroluminescent displays, indicator lights and logos, due to their comparatively high refresh rate, contrast ratio, power efficiency and capacity for vibrant colour rendering. They have broad prospects in the field of wearable devices owing to their flexibility nature, low driving voltage and low power consumption. Inkjet-printing technology has been used to date in fabricating the two key components of the device, the “frontplane” for light emitting and the “backplane” for electronic driving.

The “frontplane” of an LED includes organic light-emitting diodes (OLEDs), polymer light-emitting diodes (PLEDs) and quantum dot-based LEDs (QD LEDs). One of the major advantages of OLEDs and PLEDs is their colour-tuning capability with various emission wavelengths, which is easily obtained by changing the chemical structure of the organic compounds. Another advantage is the solution processability of the conjugated organic material, which is suitable for inkjet printing. QD LEDs are of particular interest due to their wide-ranging colour tunability, high brightness and narrow emission bandwidth. The aim is to enable patterning/stacking of red-green-blue (RGB) light-emitting materials into high-resolution, pixelated geometries with accurate control of the registration, efficient utilization of the materials and minimal chemical contamination. Thus, the inkjet-printing technique with its additive nature, compatibility with multiple material “inks” and programmable definition of patterned layouts is well-suited for the straightforward integration of multiple layers of a wearable display. Gorter *et al.* presented inkjet printing as a method to produce three active layers in a small molecule OLED stack: a hole-injection layer, a hole transport layer and an emissive layer. By modulating the printing technique, homogeneous deposition of the electro-active layers and uniform light output were achieved.²⁰³ Villani *et al.* fabricated flexible PLEDs by inkjet printing a polymer (poly(9,9-dihexyl-9H-fluorene-2,7-diyl)) as the hole-transporting layer of a hybrid structure.²⁰⁴ The device showed an optical and electrical turn-on voltage at around 8 V, which was comparable with the spin-coated one. Bulovic *et al.* demonstrated a device with patterned pixels for flexible, full-colour, large-area, AC-driven, QD-polymer-based displays

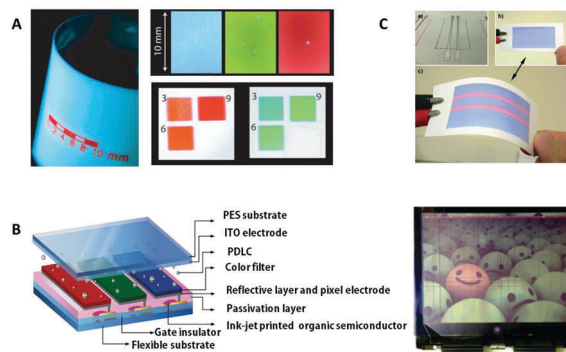


Fig. 9 (A) Left: Image showing a complete inkjet-printed AC powder electroluminescent device on a flexible substrate under $\lambda = 365$ nm wavelength illumination. Right: Images of the photoluminescence devices with different colours and layers of inkjet-printed QD-polyisobutylene (PIB). Reproduced with permission from ref. 205. Copyright 2009 Wiley. (B) Left: Scheme of one display pixel including uniform and stable printed polymer transistors array drivers for red, green and blue colour displays. Right: Image shows 4.8 inch display driven by an inkjet-printed organic thin film transistor. Reproduced with permission from ref. 100. Copyright 2013 Wiley. (C) Up: Images of the back side of blank photopaper with electrically conductive patterns and the front side of the display device inkjet printed with UV-irradiated PDA. Down: Photograph of the thermo-chromic paper display when the display is activated by supplying current through the conductive wires at the back side. The heat generated by the wires transfers to the front side and induces a blue-to-red transition on the ink-printed regions corresponding to the wires. Reproduced with permission from ref. 210. Copyright 2011 Wiley.

operating at video brightness with an efficient and robust device architecture by inkjet printing (Fig. 9A).²⁰⁵ By optimization of the QD-polymer composite layer thickness, the luminance and colour for specific applications could be modulated for improved optical and electrical performances.

The active-matrix backplane for the control of individual pixels within large arrays is also essential for wearable displays. In a simple active-matrix backplane, TFTs, which possess excellent electrical property and stability, are arrayed into rows and columns, with all the drain lines within a given column tied together and all the gate lines within a given row tied together, or *vice versa*. Depending on the application, the source of the TFTs may be either connected in series to a LED for displays or to a sensor for sensing applications. Im *et al.* inkjet-printed a large-scale, uniform and stable printed polymer transistors array with high-mobility, successfully demonstrating a high-resolution flexible colour display (Fig. 9B).¹⁰⁰ The device stability was improved by applying a surface passivation using a photoacrylate polymer resin onto inkjet-printed channels, which was anticipated to suppress the environmental effects. An organic light-emitting diode (OLED) driving circuit based on the printed TFTs was constructed by Cui's group.²⁰⁶ A single OLED was switched on with the driving circuit, showing their ability as backplanes for active-matrix OLED applications.

The light-emitting electrochemical cell (LEC) is also surface-emitting technology, but it is distinguished from the LED, since an electrolyte (mobile ions) is blended with the light-emitting compound in the active layer.²⁰⁷ The mobile ions redistribute

during LEC operation, which allows for the utilization of air-stable electrodes and a tolerance towards thick and uneven active layers.²⁰⁸ List *et al.* demonstrated an LEC display by inkjet printing an active-material ink, consisting of blends of poly[2-methoxy-5-(2-ethylhexyloxy)-1,4-phenylenevinylene] (MEH-PPV), poly(ethylene oxide) (PEO) and salt LiCF_3SO_3 , building a solid-state electrolyte.²⁰⁹ Edman *et al.* presented a novel bilayer light-emitting electrochemical cell device, comprising a patterned electrolyte in contact with a homogenous layer of a light-emitting compound as the bilayer stack.²⁷ By depositing electrolyte droplets in a well-defined binary lattice with an inkjet printer, uniform light emission with a power conversion efficacy of 0.43 lm W^{-1} , display static messages with a pixel density of 170 PPI and a high contrast were realized.

A different type of inkjet display is a thermochromic display, which has been suggested and fabricated on paper, and consists of micropatterned conducting wires on one side of a substrate and a coated thermochromic ink on the other side. When current is run through the wires, resistive heating causes the dye in the surrounding area to turn transparent. The localized heating in the substrate is claimed to be controllable to about $200 \mu\text{m}$ resolution. Thermochromic displays can be easily integrated into wearable devices that display simple messages, where a high pixel resolution is not required. Kim *et al.* constructed a prototype flexible display by utilizing the electrothermochromic property of a colorimetrically reversible polydiacetylene (PDA) composite on one side of a paper, while forming electrically conductive patterns on the opposite side (Fig. 9C).²¹⁰ When the display was activated by passing a current through the wires, the regions on the blue PDA layer corresponding to conductive patterns changed colour to red due to heat transfer from the wires to the front side of the paper containing the predefined information. Liao *et al.* fabricated wearable multi-coloured electrochromic devices by inkjet printing metallo-supramolecular polymers solutions with two primary colours on flexible electrodes.²¹¹ By digitally controlling the print dosages of each species, the colours of the printed EC thin film patterns could be adjusted directly without premixing or synthesizing new materials. The printed EC thin films were then laminated with a solid transparent thin film electrolyte and a transparent conductive thin film to form an electrochromic display.

4.2 Wearable sensors

Wearable sensors play an important role in detecting environment variations, such as stress, illumination, temperature and chemically aggressive vapours. For these applications, sensors, such as electromechanical sensors, photodetectors and chemical sensors, have been developed.^{18,212,213} With the flexibility of inkjet-printing technology, the location and circuit layouts can be adjusted easily to form a sensor. In this section, we discuss different types of sensors fabricated using inkjet printing.

Recently, inkjet-printed electromechanical sensors that can sense pressure, strain, shear forces and twist deformation for monitoring human motion (such as fingers and elbow joints movements) have attracted considerable attention. Effective signal transduction that converts external stimuli into an analog

electronic signal is an important component of accurate quantitative monitoring. Inkjet-printed electromechanical sensors rely on changes of the piezoresistivity and capacitance. Piezoresistivity-based sensors depend on piezoresistive materials, such as a conductor and semiconductor that can change their resistance under applied mechanical stress. Whitesides *et al.* fabricated piezoresistivity-based mechanical sensors with carbon ink on (3,3,4,4,5,5,6,6,7,7,8,8,9,9,10,10,10-heptadecafluorodecyl) trichlorosilane (C10F)-modified paper by an inkjet-printing method (Fig. 10A).¹²⁶ The inkjet-printed microelectromechanical systems (MEMS) deflection sensor showed a drop in resistance upon compression during upward deflection. Liu *et al.* prepared a piezoresistivity-based bending sensor by inkjet printing a blend of ink combining Ag nanowires and layered double hydroxides with a low percolation threshold on paper substrate.²¹⁴ The flexible sensor with low cost, good conductivity and sensitivity, fast response and relaxation time, extreme bending stability and nontoxicity was developed to monitor human motion. Capacitive sensors are used to measure different applied pressures or shear forces by monitoring the changes in capacitance. Holbery *et al.* fabricated a touch sensor with an inkjet-printing technique by depositing conductive PEDOT:PSS and dielectric poly(methylsiloxane) on desired areas of a flexible PET substrate, which formed a capacitive touch sensor structure (Fig. 10B).²¹⁵ Single-position and multi-touch input visualization were realized using a sensor evaluation integrated circuit board technique with embedded software. Another type of sensor is a piezoelectric-based sensor, which produces electrical charges in certain materials under mechanical force due to the occurrence of electrical dipole moments.²¹⁶ This is rarely fabricated by inkjet-printing technology but is currently undergoing rapid development to meet new challenges and opportunities that could broaden the category of inkjet-printed wearable sensors.

Photodetectors with high photosensitivity represent a crucial technology for remote control, biological health monitoring and automotive system applications.²¹⁷ Natali *et al.* reported the successful realization of flexible organic photodetectors, which exhibited a vertical topology with the photoactive layer sandwiched between two conductive stripes, by means of an inkjet-printing deposition technique (Fig. 10C).²¹⁸ Here, blends of photosensitive semiconductor P3HT and [6,6]-phenyl-C61 butyric acid methyl ester (PC61BM) were chosen as the photoactive layer. Coleman *et al.* combined the conducting material graphene and the semiconducting material MoS_2 in an all-inkjet-printed interdigitated electrode/channel structure in order to manufacture a flexible photodetector.²¹⁹ Supralinearity of the changing conductance was observed with increasing light intensity due to photocurrent quenching and the negative photoconductivity.

Wearable sensors to detect environment changes are also significant for humans to have a better comprehension of their living environment. In this regard, Liao *et al.* developed thermistor arrays for temperature-sensing applications by inkjet printing a square NiO thin film with a large temperature coefficient between two parallel silver conductive tracks on PI films.²²⁰ The inkjet-printed flexible thermistor could be bent or attached

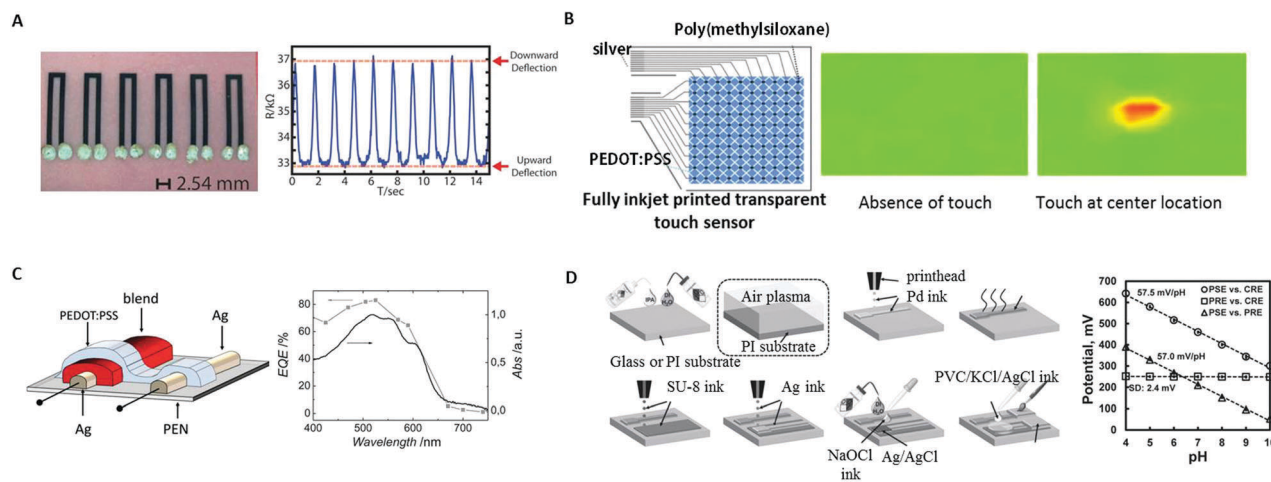


Fig. 10 (A) Left: Image of an inkjet-printed piezoresistivity type mechanical sensor. Right: Plot of resistance versus time for a representative device during 10 cycles of upward/downward deflection. Reproduced with permission from ref. 126. Copyright 2014 Wiley. (B) Left: Schematic of a transparent capacitance-type touch sensor fabricated by an inkjet-printing process. Right: Device touch sensing characterization: touch events visualization of the sensor without and with touch input at the position of intersected PEDOT:PSS electrodes. Reproduced with permission from ref. 215. Copyright 2015 American Chemical Society. (C) Left: Scheme of the inkjet printing of a flexible organic photodetector of the printed device. Right: Device photodetecting characterization: measurement of the photocurrent external quantum efficiency spectrum and normalized active layer absorbance. Reproduced with permission from ref. 218. Copyright 2013 Wiley. (D) Left: Scheme of inkjet printing an electrochemical pH sensor by integrating Pd/PdO sensing electrodes with a solid-state printed reference electrode on a PI substrate. Right: Open circuit potential versus pH values for an integrated sensor on PI. Reproduced with permission from ref. 199. Copyright 2016 Wiley.

to human skin to provide accurate and reliable temperature measurements. An inkjet-printed thermistor array was also fabricated to demonstrate the ability of printed sensors to carry out temperature distribution measurements with great precision. Deen *et al.* inkjet-printed an electrochemical pH sensor by integrating Pd/PdO sensing electrodes with a solid-state printed reference electrode on a PI substrate (Fig. 10D).¹⁹⁹ The potentiometric value was used to sense a solvent's pH due to the redox-reaction-induced ion-to-electron transduction. Since the developed sensors had high sensitivity and a fast response and were stable, low-cost and easy-to-use, a wearable electrochemical sensing platform based on inkjet printing could be built for monitoring water quality and human health conditions. Manohar *et al.* described a rugged and flexible gas sensor using inkjet-printed films comprising an all organic reduced graphene oxide (rGO)-based chemiresistor on PET to reversibly detect NO₂ and Cl₂ vapours within an air sample at the parts per billion level.²²¹ By detecting chemically aggressive vapours, human beings are able to respond rapidly towards hazardous environments.

4.3 Wearable energy devices

The rapid development of emerging wearable electronics, which is anticipated to bring unforeseen ubiquitous innovations in our daily lives, essentially requires the relentless pursuit of efficient power sources for portable self-powered devices. To power the wearable electronics, either energy storage devices or energy conversion devices can be adopted. By utilizing inkjet printing, which offers a simple and versatile route to make complicated structures, wearable energy devices can be manufactured with high efficiency and integration.²²²

Supercapacitors, serving as energy storage units, exhibit high power density, a long cycle lifespan and excellent charge-discharge and environmentally friendly characteristics despite their relative low energy densities. Inkjet-printed capacitors are currently being intensively investigated for wearable applications, such as mobile phones and flexible displays. Commonly, supercapacitors are planar-structured, with the electrolyte and the separator sandwiched by two active electrodes. Traditionally, the electrodes of a supercapacitor are inkjet-printed for patterned structures. Gao *et al.* fabricated an asymmetric supercapacitor by assembling an inkjet-printed MnO₂-Ag-MWCNT anode and a filtrated MWCNT cathode, with an electrolyte-soaked (4 M LiCl) separator infiltrated between them.²²³ The supercapacitor had a wide operating potential window of 1.8 V and exhibited excellent electrochemical performance, with a high density of 1.28 mW h cm⁻³ at a power density of 96 mW cm⁻³ and a high retention ratio of 96.9% of its initial capacitance after 3000 cycles. Huang *et al.* inkjet-printed lamellar potassium cobalt phosphate hydrate (K₂Co₃(P₂O₇)₂·2H₂O) nanocrystal whiskers (positive electrode) and graphene nanosheets (negative electrode) in order to fabricate a high-performance flexible all-solid-state asymmetric micro-supercapacitor, with solid-state KOH-PVA gel as the electrolyte.²²⁴ The micro-device offered excellent mechanical flexibility (bending angle in the range of 0°–180°), cycling stability (retaining 94.4% of capacitance after 5000 cycles) and a larger energy density (0.96 mW h cm⁻³). Due to the eco-friendly nature of the material synthesis and simple device fabrication process, the micro-device could be integrated into many wearable devices, such as power-on-chip systems and roll-up display panels. For the convenience offered through depositing the electrolyte in an accurate position in the device, all-inkjet-printed supercapacitors are also currently being investigated.

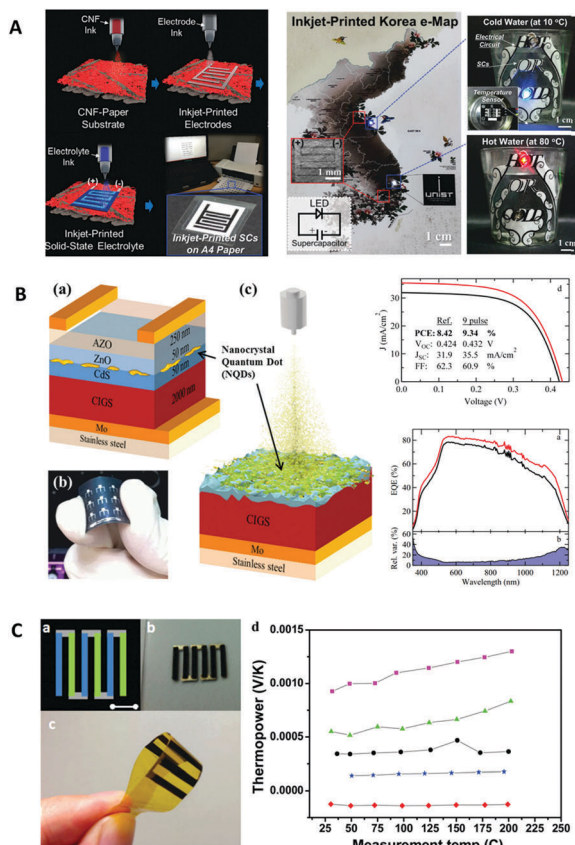


Fig. 11 (A) Left: Schematic of the stepwise fabrication procedure of inkjet-printed paper-based supercapacitors. Left: Aesthetic versatility and Internet of Things (IoT) applications of inkjet-printed supercapacitors. Reproduced with permission from ref. 225. Copyright 2016 Royal Society of Chemistry. (B) Left: Schematic and image of a flexible inkjet-printed nanocrystal quantum dots/CIGS hybrid solar cell. Right: Current–voltage and the external quantum efficiency characteristics of the device. Reproduced with permission from ref. 237. Copyright 2015 Wiley. (C) Left: Schematic and image of a printed thermoelectric generator with 3 pairs of p–n legs. Right: Graph showing the dependence of voltage with temperature. Reproduced with permission from ref. 247. Copyright 2014 Wiley.

An all-inkjet-printed, solid-state flexible supercapacitor was fabricated on paper by Lee's research group, which was composed of activated carbon/CNTs and an ionic liquid/ultraviolet-cured triacrylate polymer-based solid-state electrolyte (Fig. 11A).²²⁵ The inkjet-printed supercapacitors exhibited reliable electrochemical performance over 2000 cycles as well as good mechanical flexibility. Notably, a variety of all-inkjet-printed supercapacitors featuring computer-designed artistic patterns/letters were aesthetically unitized with other inkjet-printed images and smart glass cups, underscoring their potential applicability as an unprecedented object-tailored power source for wearable electronics.

Solar cells, which can provide more continuous energy due to their ability to constantly convert environmentally sustainable energy to electrical energy for wearable electronics, are experiencing a boost in development.^{226–228} Inkjet printing, which is utilized for the deposition of different layers of device stacks, has been investigated in the fabrication of solar cells, such as silicone solar cells,²⁰ organic solar cells,²¹ dye-sensitized

solar cells^{229,230} and perovskite solar cells.^{231,232} Since the commonly employed semi-transparent front electrode indium-tin-oxide (ITO) and F-doped SnO₂ (FTO) have several disadvantages, such as high-cost and complex vacuum deposition, a lot of studies are focused on the inkjet printing of other semi-transparent electrodes as replacements for the ITO and FTO electrode by using PEDOT:PSS²³³ or Ag current-collecting grids.²³⁴ Krebs *et al.* directly inkjet-printed semi-transparent silver grids onto flexible PET foil, followed by photonic sintering, as a front electrode, for the fabrication of organic solar cells.²³⁵ The inkjet printing of solar cell back electrodes that had no restriction of the transmission property has also been successfully demonstrated. Hasan *et al.* inkjet-printed a dye-sensitized solar cell based on pristine catalytically active and electrically conducting graphene for the fabrication of a back electrode as a Pt alternative, which limited its use on flexible substrates and in low-cost applications.²³⁶ Besides electrodes, inkjet printing is also used to produce a photoactive layer for wearable solar cells. Kuo *et al.* demonstrated inkjet-printed thin film Cu(In,Ga)Se₂ (CIGS) solar cells with self-assembled clusters of nanocrystal quantum dots, which provided a 10.9% relative enhancement of the photon conversion efficiency (Fig. 11B).²³⁷ A uniform and flat photoactive layer could be fabricated by inkjet printing.²³⁸ Song *et al.* inkjet-printed a perovskite CH₃NH₃PbI₃ layer onto a mesoporous TiO₂ substrate.²³⁹ By adjusting the printing temperature and additive agent, a flat and uniform perovskite CH₃NH₃PbI₃ film was achieved, which exhibited a power conversion efficiency of 12.3% under AM 1.5G conditions, with high reproducibility.

Thermoelectric nanogenerators have also attracted great interest as they can directly convert waste heat into electricity and *vice versa*.^{240,241} The conversion efficiency of a thermoelectric material is expressed by the dimensionless figure-of-merit (ZT), defined as $ZT = S^2T\sigma/\kappa$, where S is the Seebeck coefficient, σ is the electrical conductivity, κ is the thermal conductivity and T is the absolute temperature. A high Seebeck coefficient and high electrical conductivity combined with low thermal conductivity distinguish good thermoelectric materials.^{242,243} Inkjet-printing technology has been used in fabricating high-efficiency devices by patterning thermoelectric materials with a high ZT connected in series.²⁴⁴ Inorganic compounds with a high ZT are used for thermoelectric nanogenerators despite their brittle and scarce nature.^{245,246} Hng *et al.* fabricated flexible thin film thermoelectric devices with p-type Sb_{1.5}Bi_{0.5}Te₃ nanoparticles and n-type Bi₂Te_{2.7}Se_{0.3} nanoparticles by inkjet printing (Fig. 11C).²⁴⁷ Organic compounds have lower power conversion efficiency, but they are flexible, abundant, low-cost and solution-processable, making them suitable for inkjet printing.^{248,249} Inorganic–organic hybrid composite materials are used to increase the power conversion efficiency while maintaining the ease of processing. Besgan *et al.* achieved a thermoelectric nanogenerator with thermoelectricity in the 10 mV range and current in the μ A range by inkjet printing PEDOT:PSS/ZnO-ink as the thermoelectric materials and Ag ink as the interconnects.²⁵⁰

4.4 Other wearable devices

In addition to displays, sensors and energy devices, inkjet-printing technology can be used to fabricate other wearable devices. With an increasing dependence on wireless communication,

the demand for skin-mounted antennas that transmit and receive high-frequency signals is rapidly developing in areas such as smart phones, automotive navigation systems, wireless network systems and radio frequency identification (RFID) tags.^{251–253} To inkjet print flexible antennas with low signal loss and fast response in the high-frequency band, different inks and substrates are being investigated. Song *et al.* fabricated a RFID antenna of 6 m wireless identification by inkjet printing highly conductive and well-dispersed silver-nanoparticles-based ink.²⁵⁴ Instead of metallic ink, Nogi *et al.* overprinted metallo-organic decomposition inks onto copper foil and silver nanowire line to produce an antenna with a smooth surface. As a result, a decreased return loss at 0.5–4.0 GHz and an increased speed of data communication in a WiFi network were achieved.²⁵⁵ By patterning graphene sheets, which were derived from the reduction process of prepatterned GO using inkjet-printing technology, Jang *et al.* implemented a wide-band dipole antenna with 500 MHz bandwidth and a high transmitted power efficiency of 96.7%.²⁵⁶ As for substrates, densely packed and smooth surfaces are demanded to lower the signal loss, such as plastics²⁵⁷ and cellulose papers.²⁵⁸ To minimize the device size for convenient wearable situations, paper with a high dielectric constant was employed to shorten the length of the antenna element without affecting the radiowave frequency.²⁵⁹

Inkjet printing flexible memory devices with low write voltages, a high ON/OFF ratio and good retention characteristics and stability in ambient storage are also currently being developed. Alshareef *et al.* inkjet-printed all-polymer resistive memory devices on transparent and flexible substrates using DMSO-modified, highly conducting PEDOT:PSS as the bottom and top electrodes and an unmodified PEDOT:PSS film as the active layer. The inkjet-printed memory device was highly stable with an ON/OFF ratio $> 10^3$, a low writing voltage and excellent retention characteristics over 3 months.²⁶⁰ By using a sequence of inkjet-printing and screen-printing techniques, He *et al.* fabricated a metal-insulator-metal structure (silver/TiO₂/carbon)-based memory device with excellent rewritable switching property.¹⁷⁵ By investigating the effects of using a blocking dielectric layer and metal nanoparticles as the charge-trapping sites, Kim *et al.* inkjet-printed an array of 256-bit flexible organic nano-floating-gate memory devices on a PEN substrate.²⁶¹ This memory device in the array exhibited a high $I_{\text{on}}/I_{\text{off}}$ ($\approx 104 \pm 0.85$), a wide memory window ($\approx 43.5 \text{ V} \pm 8.3 \text{ V}$) and a high degree of reliability.

In view of these exciting progresses and ongoing efforts on inkjet-printed electronics, it is reasonable to foresee the emergence of a whole wearable system that integrates various devices in the next few years.

5. Conclusions and outlook

As a non-impact, massless, patterning approach, inkjet printing has been widely used for wearable electronics manufacturing. In this paper, technological advancements in inks, strategies and the applications of inkjet-printed wearable electronics have been summarized. Inks consisting of conductors, semiconductors and dielectrics are presented to inkjet print non-toxic, well-dispersed

and post-treatment compatible structures for wearable electronic devices. By modulating the droplet spreading, coalescence and drying process, uniform and high-resolution patterns can be inkjet-printed. In order to adapt human activity, highly flexible/stretchable substrates and other approaches are being developed. The mechanical duration of the inkjet-printed wearable devices can be prolonged, through minimizing device cracking and slipping. Furthermore, many applications, including wearable displays, wearable sensors and wearable energy devices fabricated by inkjet-printing technology, are being introduced.

Despite the above progress, there are still many challenges and opportunities in fabricating flexible/stretchable wearable electronics *via* inkjet-printing technology. Inks consisting of materials such as stretchable semiconductors²⁶² and dielectrics^{263,264} should be investigated and developed for further accelerating the realization of the rapidly developing wearable E-skin, which is required to meet the human skin mechanical compliance ($\epsilon > 100\%$, where ϵ is the strain).^{265,266} Meanwhile, apart from straight patterns, the inkjet printing of curved patterns is of great interest to broaden their application in fields such as ultra-sensitive or highly stable wearable devices.^{31,267} Furthermore, all-inkjet-printed wearable devices are highly desired, but are currently prohibited by obstacles such as incompatible interface of the different depositing inks and interval post-treatment-induced sequential inkjet printing accuracy deviation. Thus, efforts should be devoted in these areas, including investigating stable heterojunction structure formation, exploring post-treatment-free approach and designing new apparatus with higher accuracy. It is also attractive to manufacture wearable devices that are wireless and multi-functional by an all-inkjet-printing technology. The convenient and productive features of inkjet-printing technology for wearable electronics fabrication will shed light on the extensive commercialization of wearable electronics and potentially promote the desktop-printer-based homemade wearable electronics.

Acknowledgements

The authors thank the financial support of 973 Program (No. 2013CB933004), the National Nature Science Foundation (Grant No. 21671193, 51473173, 21301180, 21303218), the “Strategic Priority Research Program” of Chinese Academy of Sciences (Grant No. XDA09020000), the National Key Research and Development of China (No. 2016YFC1100500), and the collaborative Innovation Center of Green Printing & Publishing Technology (CGPT, 04190116008/002).

Notes and references

- 1 M. Ha, J. Park, Y. Lee and H. Ko, *ACS Nano*, 2015, **9**, 3421–3427.
- 2 M. Amjadi, K.-U. Kyung, I. Park and M. Sitti, *Adv. Funct. Mater.*, 2016, **26**, 1678–1698.
- 3 X. Wang, L. Dong, H. Zhang, R. Yu, C. Pan and Z. L. Wang, *Adv. Sci.*, 2015, **2**, 1500169.
- 4 T. Q. Trung and N.-E. Lee, *Adv. Mater.*, 2016, **28**, 4338–4372.

- 5 W. Zeng, L. Shu, Q. Li, S. Chen, F. Wang and X.-M. Tao, *Adv. Mater.*, 2014, **26**, 5310–5336.
- 6 M. L. Hammock, A. Chortos, B. C. K. Tee, J. B. H. Tok and Z. Bao, *Adv. Mater.*, 2013, **25**, 5997–6037.
- 7 M. Stoppa and A. Chiolerio, *Sensors*, 2014, **14**, 11957.
- 8 M. Singh, H. M. Haverinen, P. Dhagat and G. E. Jabbour, *Adv. Mater.*, 2010, **22**, 673–685.
- 9 J. Wang, L. Wang, Y. Song and L. Jiang, *J. Mater. Chem. C*, 2013, **1**, 6048–6058.
- 10 Y. Huang, W. Li, M. Qin, H. Zhou, X. Zhang, F. Li and Y. Song, *Small*, 2017, **13**, 1503339.
- 11 J. Sun, B. Bao, M. He, H. Zhou and Y. Song, *ACS Appl. Mater. Interfaces*, 2015, **7**, 28086–28099.
- 12 M. Kuang, L. Wang and Y. Song, *Adv. Mater.*, 2014, **26**, 6950–6958.
- 13 D. Tian, Y. Song and L. Jiang, *Chem. Soc. Rev.*, 2013, **42**, 5184–5209.
- 14 L. Wu, Z. Dong, F. Li, H. Zhou and Y. Song, *Adv. Opt. Mater.*, 2016, **4**, 1915–1932.
- 15 B. Kang, W. H. Lee and K. Cho, *ACS Appl. Mater. Interfaces*, 2013, **5**, 2302–2315.
- 16 P. F. Moonen, I. Yakimets and J. Huskens, *Adv. Mater.*, 2012, **24**, 5526–5541.
- 17 J. Song and H. Zeng, *Angew. Chem., Int. Ed.*, 2015, **54**, 9760–9774.
- 18 Y. S. Rim, S.-H. Bae, H. Chen, N. De Marco and Y. Yang, *Adv. Mater.*, 2016, **28**, 4415–4440.
- 19 R. G. Scalisi, M. Paleari, A. Favetto, M. Stoppa, P. Ariano, P. Pandolfi and A. Chiolerio, *Org. Electron.*, 2015, **18**, 89–94.
- 20 D. Stüwe, D. Mager, D. Biro and J. G. Korvink, *Adv. Mater.*, 2015, **27**, 599–626.
- 21 Y. Sun, Y. Zhang, Q. Liang, Y. Zhang, H. Chi, Y. Shi and D. Fang, *RSC Adv.*, 2013, **3**, 11925–11934.
- 22 B. H. Kim, M. S. Onses, J. B. Lim, S. Nam, N. Oh, H. Kim, K. J. Yu, J. W. Lee, J.-H. Kim, S.-K. Kang, C. H. Lee, J. Lee, J. H. Shin, N. H. Kim, C. Leal, M. Shim and J. A. Rogers, *Nano Lett.*, 2015, **15**, 969–973.
- 23 B. Kim, S. Jang, M. L. Geier, P. L. Prabhumirashi, M. C. Hersam and A. Dodabalapur, *Nano Lett.*, 2014, **14**, 3683–3687.
- 24 K. Jost, D. Stenger, C. R. Perez, J. K. McDonough, K. Lian, Y. Gogotsi and G. Dion, *Energy Environ. Sci.*, 2013, **6**, 2698–2705.
- 25 Z. Zhang, X. Zhang, Z. Xin, M. Deng, Y. Wen and Y. Song, *Adv. Mater.*, 2013, **25**, 6714–6718.
- 26 M. Gao, L. Li, W. Li, H. Zhou and Y. Song, *Adv. Sci.*, 2016, **3**, 1600120.
- 27 E. M. Lindh, A. Sandstroem and L. Edman, *Small*, 2014, **10**, 4148–4153.
- 28 T. Sekitani, H. Nakajima, H. Maeda, T. Fukushima, T. Aida, K. Hata and T. Someya, *Nat. Mater.*, 2009, **8**, 494–499.
- 29 A. C. Siegel, S. T. Phillips, B. J. Wiley and G. M. Whitesides, *Lab Chip*, 2009, **9**, 2775–2781.
- 30 E. Katzir, S. Yochelis, Y. Paltiel, S. Azoubel, A. Shimoni and S. Magdassi, *Sens. Actuators, B*, 2014, **196**, 112–116.
- 31 M. Su, F. Li, S. Chen, Z. Huang, M. Qin, W. Li, X. Zhang and Y. Song, *Adv. Mater.*, 2015, **28**, 1369–1374.
- 32 S. Ali, A. Hassan, G. Hassan, J. Bae and C. H. Lee, *Carbon*, 2016, **105**, 23–32.
- 33 B. Xie, C. Yang, Z. Zhang, P. Zou, Z. Lin, G. Shi, Q. Yang, F. Kang and C.-P. Wong, *ACS Nano*, 2015, **9**, 5636–5645.
- 34 S. Lee, Y. Lee, J. Park and D. Choi, *Nano Energy*, 2014, **9**, 88–93.
- 35 F. Jiao, C.-A. Di, Y. Sun, P. Sheng, W. Xu and D. Zhu, *Philos. Trans. R. Soc., A*, 2014, **372**, 20130008.
- 36 O. Reynolds, *Philos. Trans. R. Soc. London*, 1883, **174**, 935–982.
- 37 V. Bergeron, D. Bonn, J. Y. Martin and L. Vovelle, *Nature*, 2000, **405**, 772–775.
- 38 G. H. McKinley and M. Renardy, *Phys. Fluids*, 2011, **23**, 127101.
- 39 J. E. Fromm, *IBM J. Res. Dev.*, 1984, **28**, 322–333.
- 40 A. Kamysny and S. Magdassi, *Small*, 2014, **10**, 3515–3535.
- 41 J. Stegen, *J. Chem. Phys.*, 2014, **140**, 244908.
- 42 D. J. Finn, M. Lotya and J. N. Coleman, *ACS Appl. Mater. Interfaces*, 2015, **7**, 9254–9261.
- 43 Z. Yin, Y. Huang, N. Bu, X. Wang and Y. Xiong, *Chin. Sci. Bull.*, 2010, **55**, 3383–3407.
- 44 K. Kordás, T. Mustonen, G. Tóth, H. Jantunen, M. Lajunen, C. Soldano, S. Talapatra, S. Kar, R. Vajtai and P. M. Ajayan, *Small*, 2006, **2**, 1021–1025.
- 45 V. Georgakilas, A. Demeslis, E. Ntararas, A. Kouloumpis, K. Dimos, D. Gournis, M. Kocman, M. Otyepka and R. Zboril, *Adv. Funct. Mater.*, 2015, **25**, 1481–1487.
- 46 E. Gracia-Espino, G. Sala, F. Pino, N. Halonen, J. Luomahaara, J. Mäklin, G. Tóth, K. Kordás, H. Jantunen, M. Terrones, P. Heliö, H. Seppä, P. M. Ajayan and R. Vajtai, *ACS Nano*, 2010, **4**, 3318–3324.
- 47 Q. Yang, M. Deng, H. Li, M. Li, C. Zhang, W. Shen, Y. Li, D. Guo and Y. Song, *Nanoscale*, 2015, **7**, 421–425.
- 48 S. Chen, M. Su, C. Zhang, M. Gao, B. Bao, Q. Yang, B. Su and Y. Song, *Adv. Mater.*, 2015, **26**, 3928–3933.
- 49 O.-S. Kwon, H. Kim, H. Ko, J. Lee, B. Lee, C.-H. Jung, J.-H. Choi and K. Shin, *Carbon*, 2013, **58**, 116–127.
- 50 S. Azoubel, S. Shemesh and S. Magdassi, *Nanotechnology*, 2012, **23**, 344003.
- 51 J. Li, M. M. Naiini, S. Vaziri, M. C. Lemme and M. Östling, *Adv. Funct. Mater.*, 2014, **24**, 6524–6531.
- 52 H. Okimoto, T. Takenobu, K. Yanagi, Y. Miyata, H. Shimotani, H. Kataura and Y. Iwasa, *Adv. Mater.*, 2010, **22**, 3981–3986.
- 53 Y. Khan, F. J. Pavinatto, M. C. Lin, A. Liao, S. L. Swisher, K. Mann, V. Subramanian, M. M. Maharbiz and A. C. Arias, *Adv. Funct. Mater.*, 2016, **26**, 1004–1013.
- 54 K. Rajan, I. Roppolo, A. Chiappone, S. Bocchini, D. Perrone and A. Chiolerio, *Nanotechnol., Sci. Appl.*, 2016, **9**, 1.
- 55 S. Jeong, K. Woo, D. Kim, S. Lim, J. S. Kim, H. Shin, Y. Xia and J. Moon, *Adv. Funct. Mater.*, 2008, **18**, 679–686.
- 56 E. Butovsky, I. Perelshtein, I. Nissan and A. Gedanken, *Adv. Funct. Mater.*, 2013, **23**, 5794–5799.
- 57 C. Kim, G. Lee, C. Rhee and M. Lee, *Nanoscale*, 2015, **7**, 6627–6635.

- 58 S. Ma, L. Liu, V. Bromberg and T. J. Singler, *ACS Appl. Mater. Interfaces*, 2014, **6**, 19494–19498.
- 59 B. Kang, S. Han, J. Kim, S. Ko and M. Yang, *J. Phys. Chem. C*, 2011, **115**, 23664–23670.
- 60 J. Ryu, H.-S. Kim and H. T. Hahn, *J. Electron. Mater.*, 2011, **40**, 42–50.
- 61 D. Lee, D. Paeng, H. K. Park and C. P. Grigoropoulos, *ACS Nano*, 2014, **8**, 9807–9814.
- 62 M. Grouchko, A. Kamyshny, C. F. Mihailescu, D. F. Anghel and S. Magdassi, *ACS Nano*, 2011, **5**, 3354–3359.
- 63 D.-Y. Shin, M. Jung and S. Chun, *J. Mater. Chem.*, 2012, **22**, 11755–11764.
- 64 M. Abulikemu, E. H. Da'as, H. Haverinen, D. Cha, M. A. Malik and G. E. Jabbour, *Angew. Chem., Int. Ed.*, 2014, **53**, 420–423.
- 65 S. B. Walker and J. A. Lewis, *J. Am. Chem. Soc.*, 2012, **134**, 1419–1421.
- 66 C. Alessandro, B. Sergio, S. Francesco, P. Samuele, P. Denis, B. Davide, C. Mario and P. Candido Fabrizio, *Semicond. Sci. Technol.*, 2015, **30**, 104001.
- 67 A. Keawprajak, W. Koetnuyom, P. Piyakulawat, K. Jiramitmongkon, S. Pratontep and U. Asawapirom, *Org. Electron.*, 2013, **14**, 402–410.
- 68 M. Vosgueritchian, D. J. Lipomi and Z. Bao, *Adv. Funct. Mater.*, 2012, **22**, 421–428.
- 69 F. Torrisi, T. Hasan, W. Wu, Z. Sun, A. Lombardo, T. S. Kulmala, G.-W. Hsieh, S. Jung, F. Bonaccorso, P. J. Paul, D. Chu and A. C. Ferrari, *ACS Nano*, 2012, **6**, 2992–3006.
- 70 R. P. Tortorich and J.-W. Choi, *Nanomaterials*, 2013, **3**, 453–468.
- 71 A. Ciesielski and P. Samori, *Chem. Soc. Rev.*, 2014, **43**, 381–398.
- 72 E. B. Secor, P. L. Prabhmirashi, K. Puntambekar, M. L. Geier and M. C. Hersam, *J. Phys. Chem. Lett.*, 2013, **4**, 1347–1351.
- 73 T. Kim, H. Lee, J. Kim and K. S. Suh, *ACS Nano*, 2010, **4**, 1612–1618.
- 74 M. Lotya, P. J. King, U. Khan, S. De and J. N. Coleman, *ACS Nano*, 2010, **4**, 3155–3162.
- 75 E. B. Secor, B. Y. Ahn, T. Z. Gao, J. A. Lewis and M. C. Hersam, *Adv. Mater.*, 2015, **27**, 6683–6688.
- 76 J. Li, F. Ye, S. Vaziri, M. Muhammed, M. C. Lemme and M. Ostling, *Adv. Mater.*, 2013, **25**, 3985–3992.
- 77 J. Li, F. Ye, S. Vaziri, M. Muhammed, M. C. Lemme and M. Östling, *Carbon*, 2012, **50**, 3113–3116.
- 78 W. Li, F. Li, H. Li, M. Su, M. Gao, Y. Li, D. Su, X. Zhang and Y. Song, *ACS Appl. Mater. Interfaces*, 2016, **8**, 12369–12376.
- 79 D. R. Dreyer, S. Park, C. W. Bielawski and R. S. Ruoff, *Chem. Soc. Rev.*, 2010, **39**, 228–240.
- 80 L. Li, M. Gao, Y. Guo, J. Sun, Y. Li, F. Li, Y. Song and Y. Li, *J. Mater. Chem. C*, 2017, DOI: 10.1039/C1036TC05227D.
- 81 M. Neophytou, F. Hermerschmidt, A. Savva, E. Georgiou and S. A. Choulis, *Appl. Phys. Lett.*, 2012, **101**, 193302.
- 82 Y. Galagan, B. Zimmermann, E. W. C. Coenen, M. Jørgensen, D. M. Tanenbaum, F. C. Krebs, H. Gortler, S. Sabik, L. H. Slooff, S. C. Veenstra, J. M. Kroon and R. Andriessen, *Adv. Energy Mater.*, 2012, **2**, 103–110.
- 83 S. L. Wang, N. S. Liu, J. Y. Tao, C. X. Yang, W. J. Liu, Y. L. Shi, Y. M. Wang, J. Su, L. Y. Li and Y. H. Gao, *J. Mater. Chem. A*, 2015, **3**, 2407–2413.
- 84 W. Zhang, E. Bi, M. Li and L. Gao, *Colloids Surf., A*, 2016, **490**, 232–240.
- 85 A. S. Alshammari, M. Shkunov and S. R. P. Silva, *Colloid Polym. Sci.*, 2014, **292**, 661–668.
- 86 A. Denneulin, J. Bras, F. Carcone, C. Neuman and A. Blayo, *Carbon*, 2011, **49**, 2603–2614.
- 87 K. Chi, Z. Zhang, J. Xi, Y. Huang, F. Xiao, S. Wang and Y. Liu, *ACS Appl. Mater. Interfaces*, 2014, **6**, 16312–16319.
- 88 L. Li, Y. Guo, X. Zhang and Y. Song, *J. Mater. Chem. A*, 2014, **2**, 19095–19101.
- 89 A. Denneulin, J. Bras, A. Blayo, B. Khelifi, F. Roussel-Dherbey and C. Neuman, *Nanotechnology*, 2009, **20**, 385701.
- 90 Y. Sun and J. A. Rogers, *Adv. Mater.*, 2007, **19**, 1897–1916.
- 91 T. T. Baby, S. K. Garlapati, S. Dehm, M. Haeming, R. Kruk, H. Hahn and S. Dasgupta, *ACS Nano*, 2015, **9**, 3075–3083.
- 92 S. Allard, M. Forster, B. Souharce, H. Thiem and U. Scherf, *Angew. Chem., Int. Ed.*, 2008, **47**, 4070–4098.
- 93 J. E. Anthony, A. Facchetti, M. Heeney, S. R. Marder and X. Zhan, *Adv. Mater.*, 2010, **22**, 3876–3892.
- 94 Y. Wen and Y. Liu, *Adv. Mater.*, 2010, **22**, 1331–1345.
- 95 J. Doggart, Y. Wu and S. Zhu, *Appl. Phys. Lett.*, 2009, **94**, 163503.
- 96 T. M. Schmidt, T. T. Larsen-Olsen, J. E. Carle, D. Angmo and F. C. Krebs, *Adv. Energy Mater.*, 2015, **5**, 1500569.
- 97 H. Lu, J. Lin, N. Wu, S. Nie, Q. Luo, C.-Q. Ma and Z. Cui, *Appl. Phys. Lett.*, 2015, **106**, 093302.
- 98 N. D. Treat, J. A. N. Malik, O. Reid, L. Yu, C. G. Shuttle, G. Rumbles, C. J. Hawker, M. L. Chabinyk, P. Smith and N. Stingelin, *Nat. Mater.*, 2013, **12**, 628–633.
- 99 J. Kwon, S. Kyung, S. Yoon, J.-J. Kim and S. Jung, *Adv. Sci.*, 2016, **3**, 1500439.
- 100 J. Lee, D. H. Kim, J.-Y. Kim, B. Yoo, J. W. Chung, J.-I. Park, B.-L. Lee, J. Y. Jung, J. S. Park, B. Koo, S. Im, J. W. Kim, B. Song, M.-H. Jung, J. E. Jang, Y. W. Jin and S.-Y. Lee, *Adv. Mater.*, 2013, **25**, 5886–5892.
- 101 A. N. Sokolov, M. E. Roberts and Z. Bao, *Mater. Today*, 2009, **12**, 12–20.
- 102 S. K. Park, T. N. Jackson, J. E. Anthony and D. A. Mourey, *Appl. Phys. Lett.*, 2007, **91**, 063514.
- 103 R. Saito, M. Fujita, G. Dresselhaus and M. S. Dresselhaus, *Appl. Phys. Lett.*, 1992, **60**, 2204–2206.
- 104 M. S. Tang, E.-P. Ng, J. C. Juan, C. W. Ooi, T. C. Ling, K. L. Woon and P. L. Show, *Nanotechnology*, 2016, **27**, 332002.
- 105 M. S. Arnold, A. A. Green, J. F. Hulvat, S. I. Stupp and M. C. Hersam, *Nat. Nanotechnol.*, 2006, **1**, 60–65.
- 106 H. Liu, D. Nishide, T. Tanaka and H. Kataura, *Nat. Commun.*, 2011, **2**, 309.
- 107 C. Y. Khripin, J. A. Fagan and M. Zheng, *J. Am. Chem. Soc.*, 2013, **135**, 6822–6825.
- 108 Y. Hu, Y. Chen, P. Li and J. Zhang, *Small*, 2013, **9**, 1306–1311.
- 109 H. W. Lee, Y. Yoon, S. Park, J. H. Oh, S. Hong, L. S. Liyanage, H. Wang, S. Morishita, N. Patil, Y. J. Park, J. J. Park,

- A. Spakowitz, G. Galli, F. Gygi, P. H. S. Wong, J. B. H. Tok, J. M. Kim and Z. Bao, *Nat. Commun.*, 2011, **2**, 541.
- 110 H. Wang, B. Hsieh, G. Jimenez-Oses, P. Liu, C. J. Tassone, Y. Diao, T. Lei, K. N. Houk and Z. Bao, *Small*, 2015, **11**, 126–133.
- 111 A. Liscio, G. P. Veronese, E. Treossi, F. Suriano, F. Rossella, V. Bellani, R. Rizzoli, P. Samori and V. Palermo, *J. Mater. Chem.*, 2011, **21**, 2924–2931.
- 112 S. P. Singh, Z.-E. Ooi, S. N. L. Geok, G. K. L. Goh and A. Dodabalapur, *Appl. Phys. Lett.*, 2011, **98**, 073302.
- 113 S. Blumstengel, H. Glowatzki, S. Sadofev, N. Koch, S. Kowarik, J. P. Rabe and F. Henneberger, *Phys. Chem. Chem. Phys.*, 2010, **12**, 11642–11646.
- 114 D. H. Kim, H.-J. Shin, H. S. Lee, J. Lee, B.-L. Lee, W. H. Lee, J.-H. Lee, K. Cho, W.-J. Kim, S. Y. Lee, J.-Y. Choi and J. M. Kim, *ACS Nano*, 2012, **6**, 662–670.
- 115 R. P. Ortiz, A. Facchetti and T. J. Marks, *Chem. Rev.*, 2010, **110**, 205–239.
- 116 G. Vescio, J. Lopez-Vidrier, R. Leghrib, A. Cornet and A. Cirera, *J. Mater. Chem. C*, 2016, **4**, 1804–1812.
- 117 W. D. Ristenpart, P. M. McCalla, R. V. Roy and H. A. Stone, *Phys. Rev. Lett.*, 2006, **97**, 064501.
- 118 N. Kapur and P. H. Gaskell, *Phys. Rev. E: Stat., Nonlinear, Soft Matter Phys.*, 2007, **75**, 056315.
- 119 M. A. Nilsson and J. P. Rothstein, *J. Colloid Interface Sci.*, 2011, **363**, 646–654.
- 120 X. Yang, V. H. Chhasatia, J. Shah and Y. Sun, *Soft Matter*, 2012, **8**, 9205–9213.
- 121 D. Soltman and V. Subramanian, *Langmuir*, 2008, **24**, 2224–2231.
- 122 M. Liu, J. Wang, M. He, L. Wang, F. Li, L. Jiang and Y. Song, *ACS Appl. Mater. Interfaces*, 2014, **6**, 13344–13348.
- 123 M. W. Lee, N. Y. Kim, S. Chandra and S. S. Yoon, *Int. J. Multiphase Flow*, 2013, **56**, 138–148.
- 124 Y. Zhang, S. D. Oberdick, E. R. Swanson, S. L. Anna and S. Garoff, *Phys. Fluids*, 2015, **27**, 022101.
- 125 M. H. A. van Dongen, A. van Loon, R. J. Vrancken, J. P. C. Bernardis and J. F. Dijksman, *Exp. Fluids*, 2014, **55**, 1744.
- 126 J. Lessing, A. C. Glavan, S. B. Walker, C. Keplinger, J. A. Lewis and G. M. Whitesides, *Adv. Mater.*, 2014, **26**, 4677–4682.
- 127 C. Kim, M. Nogi, K. Suganuma and Y. Yamato, *ACS Appl. Mater. Interfaces*, 2012, **4**, 2168–2173.
- 128 L. Wu, Z. Dong, M. Kuang, Y. Li, F. Li, L. Jiang and Y. Song, *Adv. Funct. Mater.*, 2015, **25**, 2237–2242.
- 129 S. K. Park, D. A. Mourey, S. Subramanian, J. E. Anthony and T. N. Jackson, *Adv. Mater.*, 2008, **20**, 4145–4147.
- 130 E. Menard, M. A. Meitl, Y. Sun, J.-U. Park, D. J.-L. Shir, Y.-S. Nam, S. Jeon and J. A. Rogers, *Chem. Rev.*, 2007, **107**, 1117–1160.
- 131 K. S. Park, J. Baek, Y. Park, L. Lee, Y.-E. K. Lee, Y. Kang and M. M. Sung, *Adv. Mater.*, 2016, **28**, 2874–2880.
- 132 A. Mahajan, W. J. Hyun, S. B. Walker, J. A. Lewis, L. F. Francis and C. D. Frisbie, *ACS Appl. Mater. Interfaces*, 2015, **7**, 1841–1847.
- 133 C. E. Hendriks, P. J. Smith, J. Perelaer, A. M. J. Van den Berg and U. S. Schubert, *Adv. Funct. Mater.*, 2008, **18**, 1031–1038.
- 134 J. Z. Wang, Z. H. Zheng, H. W. Li, W. T. S. Huck and H. Sirringhaus, *Nat. Mater.*, 2004, **3**, 171–176.
- 135 P. Q. M. Nguyen, L.-P. Yeo, B.-K. Lok and Y.-C. Lam, *ACS Appl. Mater. Interfaces*, 2014, **6**, 4011–4016.
- 136 Y. Guo, L. Li, F. Li, H. Zhou and Y. Song, *Lab Chip*, 2015, **15**, 1759–1764.
- 137 S. J. Park, B. M. Weon, J. S. Lee, J. Lee, J. Kim and J. H. Je, *Nat. Commun.*, 2014, **5**, 4369.
- 138 A. Alizadeh, V. Bahadur, W. Shang, Y. Zhu, D. Buckley, A. Dhinojwala and M. Sohal, *Langmuir*, 2013, **29**, 4520–4524.
- 139 B. Bao, J. Jiang, F. Li, P. Zhang, S. Chen, Q. Yang, S. Wang, B. Su, L. Jiang and Y. Song, *Adv. Funct. Mater.*, 2015, **25**, 3286–3294.
- 140 J. Stringer and B. Derby, *J. Eur. Ceram. Soc.*, 2009, **29**, 913–918.
- 141 J. Stringer and B. Derby, *Langmuir*, 2010, **26**, 10365–10372.
- 142 T. H. J. van Osch, J. Perelaer, A. W. M. de Laat and U. S. Schubert, *Adv. Mater.*, 2008, **20**, 343–345.
- 143 B. W. An, K. Kim, M. Kim, S.-Y. Kim, S.-H. Hur and J.-U. Park, *Small*, 2015, **11**, 2263–2268.
- 144 T. Sekitani, Y. Noguchi, U. Zschieschang, H. Klauk and T. Someya, *Proc. Natl. Acad. Sci. U. S. A.*, 2008, **105**, 4976–4980.
- 145 J.-U. Park, M. Hardy, S. J. Kang, K. Barton, K. Adair, D. K. Mukhopadhyay, C. Y. Lee, M. S. Strano, A. G. Alleyne, J. G. Georgiadis, P. M. Ferreira and J. A. Rogers, *Nat. Mater.*, 2007, **6**, 782–789.
- 146 Z. Dong, J. Ma and L. Jiang, *ACS Nano*, 2013, **7**, 10371–10379.
- 147 L. Wu, Z. Dong, N. Li, F. Li, L. Jiang and Y. Song, *Small*, 2015, **11**, 4837–4843.
- 148 P. J. Yunker, T. Still, M. A. Lohr and A. G. Yodh, *Nature*, 2011, **476**, 308–311.
- 149 L. Wang, J. Wang, Y. Huang, M. Liu, M. Kuang, Y. Li, L. Jiang and Y. Song, *J. Mater. Chem.*, 2012, **22**, 21405.
- 150 W. Sempels, R. De Dier, H. Mizuno, J. Hofkens and J. Vermant, *Nat. Commun.*, 2013, **4**, 1757.
- 151 D. Kim, S. Jeong, B. K. Park and J. Moon, *Appl. Phys. Lett.*, 2006, **89**, 264101.
- 152 R. Bhardwaj, X. Fang, P. Somasundaran and D. Attinger, *Langmuir*, 2010, **26**, 7833–7842.
- 153 Z. Zhang, X. Zhang, Z. Xin, M. Deng, Y. Wen and Y. Song, *Adv. Mater.*, 2013, **25**, 6714–6718.
- 154 M. Kuang, J. Wang, B. Bao, F. Li, L. Wang, L. Jiang and Y. Song, *Adv. Opt. Mater.*, 2014, **2**, 34–38.
- 155 Y. Li, Q. Yang, M. Li and Y. Song, *Sci. Rep.*, 2016, **6**, 24628.
- 156 K. Fukuda, T. Sekine, D. Kumaki and S. Tokito, *ACS Appl. Mater. Interfaces*, 2013, **5**, 3916–3920.
- 157 H. Hu and R. G. Larson, *J. Phys. Chem. B*, 2006, **110**, 7090–7094.
- 158 R. D. Deegan, O. Bakajin, T. F. Dupont, G. Huber, S. R. Nagel and T. A. Witten, *Nature*, 1997, **389**, 827–829.
- 159 L. Wang, J. Wang, Y. Huang, M. Liu, M. Kuang, Y. Li, L. Jiang and Y. Song, *J. Mater. Chem.*, 2012, **22**, 21405–21411.
- 160 D. S. Eom, J. Chang, Y. W. Song, J. A. Lim, J. T. Han, H. Kim and K. Cho, *J. Phys. Chem. C*, 2014, **118**, 27081–27090.
- 161 L. Zhang, H. Liu, Y. Zhao, X. Sun, Y. Wen, Y. Guo, X. Gao, C.-A. Di, G. Yu and Y. Liu, *Adv. Mater.*, 2012, **24**, 436–440.

- 162 H. Wang, C. Cheng, L. Zhang, H. Liu, Y. Zhao, Y. Guo, W. Hu, G. Yu and Y. Liu, *Adv. Mater.*, 2014, **26**, 4683–4689.
- 163 A. Albrecht, A. Rivadeneyra, A. Abdellah, P. Lugli and J. F. Salmeron, *J. Mater. Chem. C*, 2016, **4**, 3546–3554.
- 164 J. Perelaer, M. Klokkenburg, C. E. Hendriks and U. S. Schubert, *Adv. Mater.*, 2009, **21**, 4830–4834.
- 165 I. Reinhold, C. E. Hendriks, R. Eckardt, J. M. Kranenburg, J. Perelaer, R. R. Baumann and U. S. Schubert, *J. Mater. Chem.*, 2009, **19**, 3384–3388.
- 166 V. Sanchez-Romaguera, S. Wunscher, B. M. Turki, R. Abbel, S. Barbosa, D. J. Tate, D. Oyeka, J. C. Batchelor, E. A. Parker, U. S. Schubert and S. G. Yeates, *J. Mater. Chem. C*, 2015, **3**, 2132–2140.
- 167 M. L. Allen, M. Aronniemi, T. Mattila, A. Alastalo, K. Ojanperä, M. Suhonen and H. Seppäm, *Nanotechnology*, 2008, **19**, 175201.
- 168 S. Jang, D. J. Lee, D. Lee and J. H. Oh, *Thin Solid Films*, 2013, **546**, 157–161.
- 169 D. Tobjork and R. Osterbacka, *Adv. Mater.*, 2011, **23**, 1935–1961.
- 170 K. Yamada, T. G. Henares, K. Suzuki and D. Citterio, *Angew. Chem., Int. Ed.*, 2015, **54**, 5294–5310.
- 171 H. Ko, J. Lee, Y. Kim, B. Lee, C.-H. Jung, J.-H. Choi, O.-S. Kwon and K. Shin, *Adv. Mater.*, 2014, **26**, 2335–2340.
- 172 T. Zhang, X. Wang, T. Li, Q. Guo and J. Yang, *J. Mater. Chem. C*, 2014, **2**, 286–294.
- 173 N. Thi Thi, M. Nogi and K. Sugauma, *J. Mater. Chem. C*, 2013, **1**, 5235–5243.
- 174 M.-C. Hsieh, C. Kim, M. Nogi and K. Sugauma, *Nanoscale*, 2013, **5**, 9289–9295.
- 175 D.-H. Lien, Z.-K. Kao, T.-H. Huang, Y.-C. Liao, S.-C. Lee and J.-H. He, *ACS Nano*, 2014, **8**, 7613–7619.
- 176 G. Grau, R. Kitsomboonloha, S. L. Swisher, H. Kang and V. Subramanian, *Adv. Funct. Mater.*, 2014, **24**, 5067–5074.
- 177 H. M. Lee, H. B. Lee, D. S. Jung, J.-Y. Yun, S. H. Ko and S. B. Park, *Langmuir*, 2012, **28**, 13127–13135.
- 178 A. Chauraya, W. G. Whittow, J. C. Vardaxoglou, Y. Li, R. Torah, K. Yang, S. Beeby and J. Tudor, *IET Microw. Antennas Propag.*, 2013, **7**, 760–767.
- 179 P. Chen, H. Chen, J. Qiu and C. Zhou, *Nano Res.*, 2010, **3**, 594–603.
- 180 B. Hu, D. Li, P. Manandhar, Q. Fan, D. Kasilingam and P. Calvert, *J. Mater. Chem.*, 2012, **22**, 1598–1605.
- 181 B. Hu, D. Li, O. Ala, P. Manandhar, Q. Fan, D. Kasilingam and P. D. Calvert, *Adv. Funct. Mater.*, 2011, **21**, 305–311.
- 182 W. G. Whittow, A. Chauraya, J. C. Vardaxoglou, Y. Li, R. Torah, K. Yang, S. Beeby and J. Tudor, *IEEE Antennas Wirel. Propag. Lett.*, 2014, **13**, 71–74.
- 183 Z. Stempien, E. Rybicki, T. Rybicki and J. Lesnikowski, *Sens. Actuators, B*, 2016, **224**, 714–725.
- 184 T. Cheng, Y. Z. Zhang, W. Y. Lai and W. Huang, *Adv. Mater.*, 2015, **27**, 3349–3376.
- 185 S. Yao and Y. Zhu, *Adv. Mater.*, 2015, **27**, 1480–1511.
- 186 T. Q. Trung and N.-E. Lee, *Adv. Mater.*, 2017, **29**, 1603167.
- 187 H. Wu, Y. Huang, F. Xu, Y. Duan and Z. Yin, *Adv. Mater.*, 2016, **28**, 9881–9919.
- 188 A. Vohra, H. L. Filiatrault, S. D. Amyotte, R. S. Carmichael, N. D. Suhan, C. Siegers, L. Ferrari, G. J. E. Davidson and T. B. Carmichael, *Adv. Funct. Mater.*, 2016, **26**, 5222–5229.
- 189 T. Kim, H. Song, J. Ha, S. Kim, D. Kim, S. Chung, J. Lee and Y. Hong, *Appl. Phys. Lett.*, 2014, **104**, 113103.
- 190 S. Chung, J. Lee, H. Song, S. Kim, J. Jeong and Y. Hong, *Appl. Phys. Lett.*, 2011, **98**, 153110.
- 191 J. Lee, S. Chung, H. Song, S. Kim and Y. Hong, *J. Phys. D: Appl. Phys.*, 2013, **46**, 5.
- 192 M. Park, J. Im, M. Shin, Y. Min, J. Park, H. Cho, S. Park, M.-B. Shim, S. Jeon, D.-Y. Chung, J. Bae, J. Park, U. Jeong and K. Kim, *Nat. Nanotechnol.*, 2012, **7**, 803–809.
- 193 S. Kim, J. Byun, S. Choi, D. Kim, T. Kim, S. Chung and Y. Hong, *Adv. Mater.*, 2014, **26**, 3094–3099.
- 194 R. Guo, Y. Yu, Z. Xie, X. Liu, X. Zhou, Y. Gao, Z. Liu, F. Zhou, Y. Yang and Z. Zheng, *Adv. Mater.*, 2013, **25**, 3343–3350.
- 195 V. Sanchez-Romaguera, M. B. Madec and S. G. Yeates, *React. Funct. Polym.*, 2008, **68**, 1052–1058.
- 196 A. Russo, B. Y. Ahn, J. J. Adams, E. B. Duoss, J. T. Bernhard and J. A. Lewis, *Adv. Mater.*, 2011, **23**, 3426–3430.
- 197 A. Mahajan, L. F. Francis and C. D. Frisbie, *ACS Appl. Mater. Interfaces*, 2014, **6**, 1306–1312.
- 198 W. Huang, K. Besar, Y. Zhang, S. Yang, G. Wiedman, Y. Liu, W. Guo, J. Song, K. Hemker, K. Hristova, I. J. Kymissis and H. E. Katz, *Adv. Funct. Mater.*, 2015, **25**, 3745–3755.
- 199 Y. Qin, A. U. Alam, M. M. R. Howlader, N.-X. Hu and M. J. Deen, *Adv. Funct. Mater.*, 2016, **26**, 4923–4933.
- 200 A. Chiolerio, P. Rivolo, S. Porro, S. Stassi, S. Ricciardi, P. Mandracci, G. Canavese, K. Bejtka and C. F. Pirri, *RSC Adv.*, 2014, **4**, 51477–51485.
- 201 J. Jiang, B. Bao, M. Li, J. Sun, C. Zhang, Y. Li, F. Li, X. Yao and Y. Song, *Adv. Mater.*, 2016, **28**, 1420–1426.
- 202 M. D. Thouless, *J. Vac. Sci. Technol., A*, 1991, **9**, 2510–2515.
- 203 H. Gorter, M. J. J. Coenen, M. W. L. Slaats, M. Ren, W. Lu, C. J. Kuijpers and W. A. Groen, *Thin Solid Films*, 2013, **532**, 11–15.
- 204 F. Villani, P. Vacca, G. Nenna, O. Valentino, G. Burrasca, T. Fasolino, C. Minarini and D. della Sala, *J. Phys. Chem. C*, 2009, **113**, 13398–13402.
- 205 V. Wood, M. J. Panzer, J. Chen, M. S. Bradley, J. E. Halpert, M. C. Bawendi and V. Bulovic, *Adv. Mater.*, 2009, **21**, 2151–2155.
- 206 W. Xu, J. Zhao, L. Qian, X. Han, L. Wu, W. Wu, M. Song, L. Zhou, W. Su, C. Wang, S. Nie and Z. Cui, *Nanoscale*, 2014, **6**, 1589–1595.
- 207 A. Sandström and L. Edman, *Energy Technol.*, 2015, **3**, 329–339.
- 208 J. Liang, L. Li, X. Niu, Z. Yu and Q. Pei, *Nat. Photonics*, 2013, **7**, 817–824.
- 209 G. Mauthner, K. Landfester, A. Köck, H. Brückl, M. Kast, C. Stepper and E. J. W. List, *Org. Electron.*, 2008, **9**, 164–170.
- 210 B. Yoon, D.-Y. Ham, O. Yarimaga, H. An, C. W. Lee and J.-M. Kim, *Adv. Mater.*, 2011, **23**, 5492–5497.

- 211 B.-H. Chen, S.-Y. Kao, C.-W. Hu, M. Higuchi, K.-C. Ho and Y.-C. Liao, *ACS Appl. Mater. Interfaces*, 2015, **7**, 25069–25076.
- 212 Z. Fan, J. C. Ho, T. Takahashi, R. Yerushalmi, K. Takei, A. C. Ford, Y.-L. Chueh and A. Javey, *Adv. Mater.*, 2009, **21**, 3730–3743.
- 213 K. Chen, W. Gao, S. Emaminejad, D. Kiriya, H. Ota, H. Y. Y. Nyein, K. Takei and A. Javey, *Adv. Mater.*, 2016, **28**, 4397–4414.
- 214 Y. Wei, S. Chen, F. Li, Y. Lin, Y. Zhang and L. Liu, *ACS Appl. Mater. Interfaces*, 2015, **7**, 14182–14191.
- 215 S. Ma, F. Ribeiro, K. Powell, J. Lutian, C. Moller, T. Large and J. Holbery, *ACS Appl. Mater. Interfaces*, 2015, **7**, 21628–21633.
- 216 M. Gao, L. Li, W. Li, H. Zhou and Y. Song, *Adv. Sci.*, 2016, **3**, 1600120.
- 217 Z. Lou and G. Shen, *Adv. Sci.*, 2016, **3**, 1500287.
- 218 G. Azzellino, A. Grimoldi, M. Binda, M. Caironi, D. Natali and M. Sampietro, *Adv. Mater.*, 2013, **25**, 6829–6833.
- 219 D. J. Finn, M. Lotya, G. Cunningham, R. J. Smith, D. McCloskey, J. F. Donegan and J. N. Coleman, *J. Mater. Chem. C*, 2014, **2**, 925–932.
- 220 C.-C. Huang, Z.-K. Kao and Y.-C. Liao, *ACS Appl. Mater. Interfaces*, 2013, **5**, 12954–12959.
- 221 V. Dua, S. P. Surwade, S. Ammu, S. R. Agnihotra, S. Jain, K. E. Roberts, S. Park, R. S. Ruoff and S. K. Manohar, *Angew. Chem., Int. Ed.*, 2010, **49**, 2154–2157.
- 222 S. Lawes, A. Riese, Q. Sun, N. Cheng and X. Sun, *Carbon*, 2015, **92**, 150–176.
- 223 S. Wang, N. Liu, J. Tao, C. Yang, W. Liu, Y. Shi, Y. Wang, J. Su, L. Li and Y. Gao, *J. Mater. Chem. A*, 2015, **3**, 2407–2413.
- 224 H. Pang, Y. Zhang, W.-Y. Lai, Z. Hu and W. Huang, *Nano Energy*, 2015, **15**, 303–312.
- 225 K.-H. Choi, J. Yoo, C. K. Lee and S.-Y. Lee, *Energy Environ. Sci.*, 2016, **9**, 2812–2821.
- 226 M. A. Green, A. Ho-Baillie and H. J. Snaith, *Nat. Photonics*, 2014, **8**, 506–514.
- 227 P. Docampo, S. Guldin, T. Leijtens, N. K. Noel, U. Steiner and H. J. Snaith, *Adv. Mater.*, 2014, **26**, 4013–4030.
- 228 Q. An, F. Zhang, J. Zhang, W. Tang, Z. Deng and B. Hu, *Energy Environ. Sci.*, 2016, **9**, 281–322.
- 229 S. G. Hashmi, M. Ozkan, J. Halme, K. D. Misic, S. M. Zakeeruddin, J. Paltakari, M. Graetzel and P. D. Lund, *Nano Energy*, 2015, **17**, 206–215.
- 230 R. Cherrington, D. J. Hughes, S. Senthilarasu and V. Goodship, *Energy Technol.*, 2015, **3**, 866–870.
- 231 A. Mei, X. Li, L. Liu, Z. Ku, T. Liu, Y. Rong, M. Xu, M. Hu, J. Chen, Y. Yang, M. Grätzel and H. Han, *Science*, 2014, **345**, 295–298.
- 232 Z. Wei, H. Chen, K. Yan and S. Yang, *Angew. Chem., Int. Ed.*, 2014, **53**, 13239–13243.
- 233 A. Singh, M. Katiyar and A. Garg, *RSC Adv.*, 2015, **5**, 78677–78685.
- 234 Y. Galagan, B. Zimmermann, E. W. C. Coenen, M. Jorgensen, D. M. Tanenbaum, F. C. Krebs, H. Gortler, S. Sabik, L. H. Slooff, S. C. Veenstra, J. M. Kroon and R. Andriessen, *Adv. Energy Mater.*, 2012, **2**, 103–110.
- 235 D. Angmo, T. T. Larsen-Olsen, M. Jorgensen, R. R. Sondergaard and F. C. Krebs, *Adv. Energy Mater.*, 2013, **3**, 172–175.
- 236 D. Dodoo-Arhin, R. C. T. Howe, G. Hu, Y. Zhang, P. Hiralal, A. Bello, G. Amaratunga and T. Hasan, *Carbon*, 2016, **105**, 33–41.
- 237 Y.-K. Liao, M. Brossard, D.-H. Hsieh, T.-N. Lin, M. D. B. Charlton, S.-J. Cheng, C.-H. Chen, J.-L. Shen, L.-T. Cheng, T.-P. Hsieh, F.-I. Lai, S.-Y. Kuo, H.-C. Kuo, P. G. Savvidis and P. G. Lagoudakis, *Adv. Energy Mater.*, 2015, **5**, 1401280.
- 238 P. Li, C. Liang, Y. Zhang, F. Li, Y. Song and G. Shao, *ACS Appl. Mater. Interfaces*, 2016, **8**, 32574–32580.
- 239 S.-G. Li, K.-J. Jiang, M.-J. Su, X.-P. Cui, J.-H. Huang, Q.-Q. Zhang, X.-Q. Zhou, L.-M. Yang and Y.-L. Song, *J. Mater. Chem. A*, 2015, **3**, 9092–9097.
- 240 R. Kroon, D. A. Mengistie, D. Kiefer, J. Hynynen, J. D. Ryan, L. Yu and C. Muller, *Chem. Soc. Rev.*, 2016, **45**, 6147–6164.
- 241 Q. Zhang, Y. Sun, W. Xu and D. Zhu, *Adv. Mater.*, 2014, **26**, 6829–6851.
- 242 D. L. Medlin and G. J. Snyder, *Curr. Opin. Colloid Interface Sci.*, 2009, **14**, 226–235.
- 243 M. S. Dresselhaus, G. Chen, M. Y. Tang, R. G. Yang, H. Lee, D. Z. Wang, Z. F. Ren, J. P. Fleurial and P. Gogna, *Adv. Mater.*, 2007, **19**, 1043–1053.
- 244 M. Orrill and S. LeBlanc, *J. Appl. Polym. Sci.*, 2017, **134**, 44256.
- 245 L. J. Hoong, Y. C. Keat, A. Chik and T. P. Leng, *Ceram. Int.*, 2016, **42**, 12064–12073.
- 246 X. Yan, B. Poudel, Y. Ma, W. S. Liu, G. Joshi, H. Wang, Y. Lan, D. Wang, G. Chen and Z. F. Ren, *Nano Lett.*, 2010, **10**, 3373–3378.
- 247 Z. Lu, M. Layani, X. Zhao, L. P. Tan, T. Sun, S. Fan, Q. Yan, S. Magdassi and H. H. Hng, *Small*, 2014, **10**, 3551–3554.
- 248 O. Bubnova, Z. U. Khan, A. Malti, S. Braun, M. Fahlman, M. Berggren and X. Crispin, *Nat. Mater.*, 2011, **10**, 429–433.
- 249 Y. Sun, P. Sheng, C. Di, F. Jiao, W. Xu, D. Qiu and D. Zhu, *Adv. Mater.*, 2012, **24**, 932–937.
- 250 A. Besgan, V. Zöllmer, R. Kun, E. Pál, L. Walder and M. Busse, *Procedia Technol.*, 2014, **15**, 99–106.
- 251 V. Sanchez-Romaguera, S. Wuenscher, B. M. Turki, R. Abbel, S. Barbosa, D. J. Tate, D. Oyeka, J. C. Batchelor, E. A. Parker, U. S. Schubert and S. G. Yeates, *J. Mater. Chem. C*, 2015, **3**, 2132–2140.
- 252 M. Kubo, X. Li, C. Kim, M. Hashimoto, B. J. Wiley, D. Ham and G. M. Whitesides, *Adv. Mater.*, 2010, **22**, 2749–2752.
- 253 S. Cheng, A. Rydberg, K. Hjort and Z. Wu, *Appl. Phys. Lett.*, 2009, **94**, 144103.
- 254 Z. Zhang, X. Zhang, Z. Xin, M. Deng, Y. Wen and Y. Song, *Nanotechnology*, 2011, **22**, 425601.
- 255 N. Komoda, M. Nogi, K. Sugauma and K. Otsuka, *ACS Appl. Mater. Interfaces*, 2012, **4**, 5732–5736.
- 256 K.-Y. Shin, J.-Y. Hong and J. Jang, *Adv. Mater.*, 2011, **23**, 2113–2118.
- 257 Y.-L. Tai and Z.-G. Yang, *ACS Appl. Mater. Interfaces*, 2015, **7**, 17104–17111.
- 258 M. Nogi, N. Komoda, K. Otsuka and K. Sugauma, *Nanoscale*, 2013, **5**, 4395–4399.

- 259 T. Inui, H. Koga, M. Nogi, N. Komoda and K. Suganuma, *Adv. Mater.*, 2015, **27**, 1112–1116.
- 260 U. S. Bhansali, M. A. Khan, D. Cha, M. N. AlMadhoun, R. Li, L. Chen, A. Amassian, I. N. Odeh and H. N. Alshareef, *ACS Nano*, 2013, **7**, 10518–10524.
- 261 M. Kang, K.-J. Baeg, D. Khim, Y.-Y. Noh and D.-Y. Kim, *Adv. Funct. Mater.*, 2013, **23**, 3503–3512.
- 262 S. J. Benight, C. Wang, J. B. H. Tok and Z. Bao, *Prog. Polym. Sci.*, 2013, **38**, 1961–1977.
- 263 D. Kong, R. Pfattner, A. Chortos, C. Lu, A. C. Hinckley, C. Wang, W.-Y. Lee, J. W. Chung and Z. Bao, *Adv. Funct. Mater.*, 2016, **26**, 4680–4686.
- 264 A. Chortos, J. Lim, J. W. F. To, M. Vosgueritchian, T. J. Dusseault, T.-H. Kim, S. Hwang and Z. Bao, *Adv. Mater.*, 2014, **26**, 4253–4259.
- 265 N. Lu, C. Lu, S. Yang and J. Rogers, *Adv. Funct. Mater.*, 2012, **22**, 4044–4050.
- 266 M. Amjadi, Y. J. Yoon and I. Park, *Nanotechnology*, 2015, **26**, 375501.
- 267 J. A. Fan, W.-H. Yeo, Y. Su, Y. Hattori, W. Lee, S.-Y. Jung, Y. Zhang, Z. Liu, H. Cheng, L. Falgout, M. Bajema, T. Coleman, D. Gregoire, R. J. Larsen, Y. Huang and J. A. Rogers, *Nat. Commun.*, 2014, **5**, 3266.